Optics and Lasers in Engineering 135 (2020) 106191

Contents lists available at ScienceDirect

Optics and Lasers in Engineering

journal homepage: www.elsevier.com/locate/optlaseng

Recent advances in optical tomography in low scattering media

Asier Marcos-Vidal[a,*], Jorge Ripoll[a,b]

[a] Departament of Bioengineering and Aerospace Engineering, Universidad Carlos III de Madrid, 28911 Leganés, Madrid, Spain
[b] Experimental Medicine and Surgery Unit, Instituto de Investigación Sanitaria Gregorio Marañón, 28007 Madrid, Spain

ARTICLE INFO

Keywords:
Light sheet microscopy
SPIM
DSLM
Optical projection tomography
OPT
Optical imaging

ABSTRACT

Low scattering media is the best scenario for optical imaging in thick samples and deep tissue, as it allows to obtain high resolution images without suffering the limitations that the diffusion phenomenon imposes. The high contribution of ballistic light in this regime enabled the development of light sheet microscopy and optical projection tomography, two of the most common techniques nowadays in research laboratories. Their revolutionary approach and wide spectrum of applications and possibilities has lead to a frenetic rhythm of new works and techniques arising every year. The large amount of information available often overwhelms scientists and researchers trying to keep up to date with the last cutting edge advances of the field. This paper aims to give a brief review of the origins and fundamental aspects of these two techniques to focus on the most recent and yet non reviewed works. Apart from novel methods, this document also covers combined multimodal approaches and systems. To conclude, we put a spotlight on the important role that open-source microscopy systems play in the field, as they improve the accessibility to these techniques and promote collaborative networks across the optical imaging community.

1. Introduction

The study of biological processes at microscopic scale cannot be conceived without resorting to optical imaging. This tool allowed researchers to reveal some of the best kept secrets of nature, hidden in the vast invisible world beyond the limits of our naked eyes. Optical microscopy arose in the 17th century but it was just a few decades ago, with the arrival of computers and digital sensors, that the revolution in which we will focus on here began. New technologies have permitted great advances in the field, passing from widefield two dimensional grey scale images to systems capable of capturing deep tissue diffraction limited images in a very short period of time. These advances in the field of optical microscopy have been made possible with large investments of time and resources, together with the most ingenious ideas from a large community of scientists driven by curiosity and yearn for new technologies and discoveries.

Three dimensional imaging is one of the main recent achievements of optical microscopy, which allows to study large and complex structures with cellular resolution. During the last twenty years, since the spread of Confocal Microscopy [1], and with the arrival of new techniques such as Optical Projection Tomography (OPT) or Light Sheet Fluorescence Microscopy (LSFM), imaging systems can obtain meaningful high resolution and depth resolved images of a sample, in some cases with temporal resolution. However, despite the most recent advances have achieved impressive qualitative improvements, the physics of light propagation still constrains the applications in which these modalities can be used.

Image quality when studying biological tissue strongly relies on the degree of transparency of the sample. Absorption, due to the presence of chromophores, limits the penetration of light, and scattering, due to the heterogeneous refraction index of tissues, reduces drastically the resolution of the images. Generally, biological tissue is considered a highly scattering medium, meaning that light propagates without deviating from its original path (i.e. ballistically), for just a few hundred of microns [2]. Above this limit, the effects of scattering become stronger until the propagation regime falls into the diffusion model [3], where there are no remainders of ballistic light and thus the propagation is locally equivalent to light paths describing random walks.

Since samples for OPT and LSFM either have sizes below the diffusion barrier or undergo chemical clearing, the imaging process presumably occurs within the ballistic domain. This assumption enables to reconstruct the images using the inverse radon transform [4] or to propagate a thin sheet of light for up to several millimeters. These two techniques take advantage of the forward propagation of light within short distances to acquire high resolution images, however, as the transition between regimes doesn't occur abruptly, strategies to mitigate the weaker effects of scattering must be designed. This is specially significant for small in vivo or large size cleared samples, where the degradation of the image at certain depths is more noticeable.

* Corresponding author.
E-mail addresses: asmarcos@ing.uc3m.es (A. Marcos-Vidal), jorge.ripoll@uc3m.es (J. Ripoll).

https://doi.org/10.1016/j.optlaseng.2020.106191
Received 26 October 2019; Received in revised form 5 May 2020; Accepted 11 May 2020
Available online 15 June 2020

The strong impact of LSFM and OPT in the microscopy community has led to a frenetic rhythm of new works and publications that often overwhelms researchers trying to stay up to date with the latest cutting edge developments. There are many comprehensive reviews in the literature describing the evolution these techniques and their variants with all degrees of technical details [5–10]. In addition, given the large amount of applications they can be used for, there are focused reviews on specific research fields such as neuroscience [11], developmental processes [12], imaging combined with microdevices and fuidics [13], histopathology [14], study of protein dynamics [15], mammalian development [16], super-resolution imaging in mammalian cells [17], live plants [18], and biological studies [19]. This review paper aims to cover the fundamental aspects of OPT and LSFM and will focus on the most recent advances from both techniques over the last few years.

2. Optical projection tomography

Optical Projection Tomography (OPT) is an optical imaging technique that measures the three dimensional distribution of the absorption or the fluorochromes in small specimens non invasively [20]. This technique is the optical counterpart of x-ray tomography and therefore its imaging process consists of an acquisition part, where a set of images from the sample named projections are captured from several angular positions, and a reconstruction procedure, where a three dimensional map of the measurement is generated using a mathematical model. The acquisition can be made in fluorescence mode, exciting the whole sample simultaneously with an LED, or in transillumination, measuring the transmitted light through the specimen.

Standard OPT assumes that samples are optically transparent and thus scattering is negligible. In fact, the reconstruction algorithm used for this technique, the filtered backprojection (FBP) [4], performs an inverse Radon transform as in x-ray CT. Therefore, intensity values in each pixel of the projections represent the line integral of the magnitude being measured along the normal direction to the projection plane. As a consequence, the use of OPT in turbid samples would not match this propagation model, causing a dramatic loss of resolution in the images [21,22].

2.1. Setup and acquisition methods

The classical setup in transmission OPT uses an incoherent light source to illuminate a specimen that is usually embedded in an immersion medium and is mounted in a rotating stage [20]. The illumination in OPT is usually delivered using a regular illuminator, which consists of a LED and a diffuser [23]. More complex setups can be implemented in order to ensure homogeneous illumination and control of the delivered intensity. These can include collimation optics [24] such as telecentric illumination lenses [25] or a Köhler illuminator [26]. At the other end, a camera with an objective lens of very reduced numerical aperture (NA) accepts only rays traveling in the parallel direction to the optical axis and captures the transmitted light. In the case of operating in fluorescence mode, the illuminator can be reduced to a simple LED source. Also, in this case a detection filter should be placed in front of the sensor to discard the excitation light (see Fig. 1).

As in other optical imaging techniques, the choice of objective lens is very important in OPT. Lenses should be able to reject scattered photons, have a long depth of field (DOF) to capture thick samples in focus, large field of view (FOV) and high resolution.

It is well known in optics that low NA objective lenses have long DOF at the cost of losing resolution, therefore a compromise must be found. The resolution limit of low NA optics is specially relevant with small samples since mesoscopic imaging systems are often limited by the pixel size of the camera sensor. If the DOF is not sufficient to keep the entire sample depth in focus, the recommendation is to set the focal plane at the first half of the sample, having at least this region in sharp focus [27]. The DOF can be synthetically extended in OPT by performing axial scanning with a piezo electric positioner in the detection objective lens [28] or, for faster acquisition times, with an electrically tunable lens (ETL)[29]. Finally, it is worthwhile to mention that it is also desirable to have objective lenses with high telecentricity to avoid image distortion and to have better discrimination of the parallel rays to the optical axis [30,31].

The choice of NA of the objective lens can reduce non desired scattered light. In fact, extremely low NA lenses can enable the localization of fluorescent probes in large sized no cleared samples of up to a cm diameter [32]. Alternatively, time gating has been also suggested as a way to perform this task, as non scattered photons travel shorter paths and arrive earlier to the camera sensor. Time-gated OPT exploits this effect using a high temporal resolution detector [33]. This method was used to image an adult zebrafish [34] resolving the internal structure without any previous clearing process, demonstrating higher contrast and less artifacts in the reconstructions. This method, although can significantly improve the quality of the images, in large sized or highly scattering samples may restrict sensitivity of the system, dropping the signal to noise ratio unless the acquisition time is increased. Recently, a simulation study based on the Monte Carlo method [35] concluded that time domain detection has larger margin of image contrast improvement than angular rejection [36]. This may be explained through the fact that time-gating performs real scattering rejection whereas angular rejection may capture scattered waves that eventually end up propagating parallel to the optical axis.

Since the use of low NA objective lenses reduces the collection efficiency of the system, especially in fluorescence mode due to the isotropic profile of the sources, some groups have proposed alternative OPT implementations. Scanning Laser Optical Tomography (SLOT) [37] uses photodetectors instead of a camera to extend the dynamic range and the detection efficiency. In this technique, a galvomirror sweeps the beam to scan the specimen. Collection can be made in transmission with a photodiode placed behind the sample on the optical axis or in fluorescence with a lens system and a photomultiplier that captures autofluorescence from the orthogonal direction. This method allows to increase significantly the signal to noise ratio of the projections since the detection technology used here offers better sensitivity than a camera sensor. Furthermore, illuminating with a focused beam allows to deliver higher power to the tissues, enabling Second Harmonic Generation (SHG) [38] imaging in this technique.

Increasing the dynamic range of the system can be beneficial in cases where there is a large range of absorption rates in the sample tissues. Adjusting the exposure of the camera is usually a straight forward process with transparent samples. However, in highly absorbing specimens light might saturate projections in the areas of the image where the sample has thinner cross-sections or yield unexposed areas in the thicker ones. Apart from using photodetectors, which is much slower and complicated in terms of acquisition time and alignment, high dynamic range (HDR) fusion has also been suggested to extend the dynamic range of the images [39]. While this approach seems adequate to image highly absorbing samples with correct exposure across the whole image, the quantification of the absorption may turn complicated since images are merged using computational algorithms.

2.2. Advanced reconstruction techniques

The standard algorithm for the Radon inverse transform does not consider most of the particularities of the physics of optical systems in respect to the x-ray propagation model. The characteristics and optical performance of the lenses, the optical properties of the sample or the mismatch between the indices of refraction at the different interfaces along the optical paths are critical factors that degrade the quality of the images. Reconstructions can be improved by including more sophisticated models in the kernel or by performing specific post or preprocessing to the images. Since the output of an OPT system is the result of convolving the sample's 3D distribution of the measured magnitude

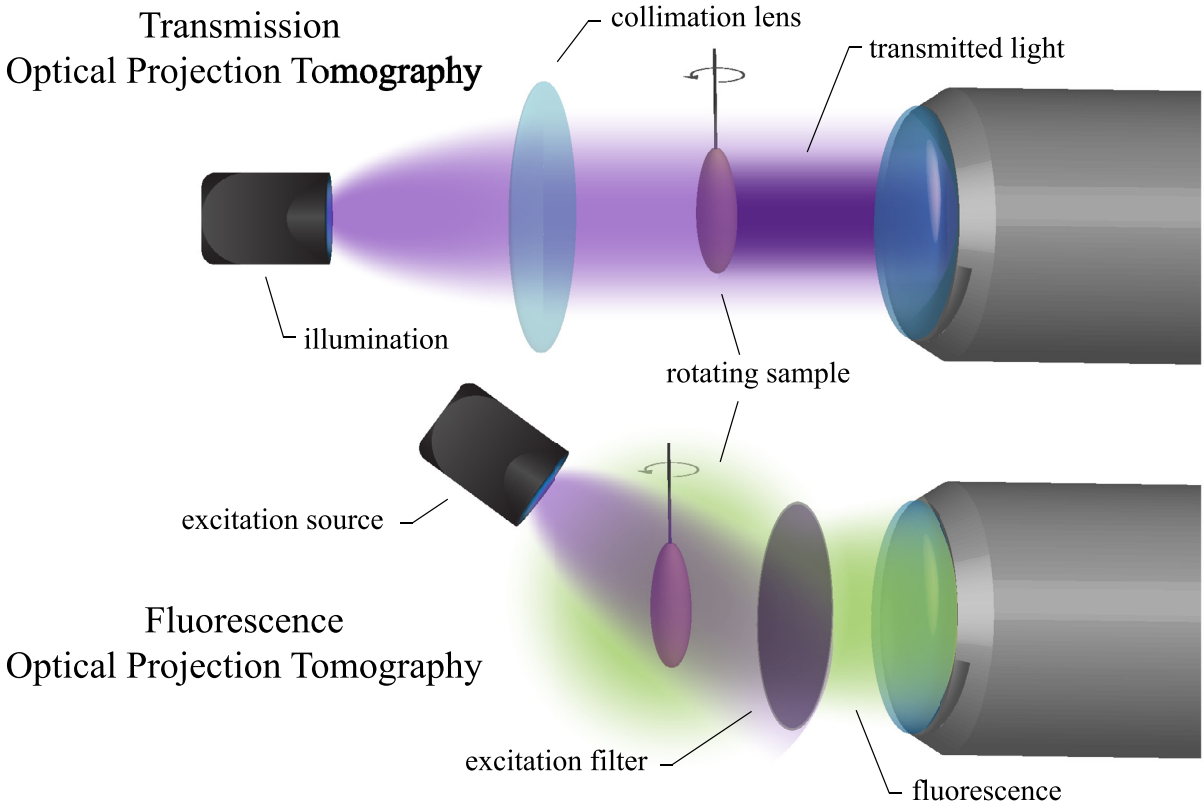

Fig. 1. Transmission OPM (top) illuminates the sample with collimated light and captures the transmitted intensity. Fluorescence OPT (bottom) excites the samples with a source and collects the emitted fluorescence. In both modes the sample is rotated to acquire images from several views.

with the point spread function (PSF) of the optics and the medium, deconvolution techniques can be applied to the sinograms prior to the FBP or as a postprocessing step after the reconstruction [40]. Whereas these methods can significantly improve the resolution of the reconstructions, the results strongly depend on the choice of algorithm, and require fine tuning of their parameters in order to avoid amplifying the noise level in the output.

Preprocessing of the tomograms has demonstrated to be an effective technique to reduce blurriness from scattering by estimating the PSF of a point source placed at the center of the volume. This information can be used to deconvolve the projections before the reconstruction [41]. In a similar way, lens defocusing can be also compensated to improve the resolution isotropy across the FOV in the reconstructed volume [42]. The resolution loss in regions far from the center of the FOV caused by the imaging optics can be also addressed through deconvolution if a frequency domain analysis of the image resolution is performed to characterize the system [43].

This methods usually use iterative reconstruction algorithms to solve the minimization problem and have been successfully employed in several works to account for the PSF of the optics [44,45]. A recent study presented a comparison among several deconvolution and reconstruction strategies, concluding that these techniques provide better results than simple FBP, being PSF based reconstructions the best, specially in systems where its PSF cannot be described analytically [40]. Also, for isotropic sources as in fluorescence mode, models have been developed to account for this special emission geometry using a weighted FBP [46].

Tomographic reconstruction assumes a perfect geometry of the scanner, where rotation occurs smoothly and there are no misalignments of the system, mechanical vibrations or defective elements in the camera sensor. Deviations from this model will produce artifacts in the reconstructed images such as double edges in structure boundaries, blurriness or rings in the axial slices. In order to obtain the best image quality, these nonidealities need to be accounted during the reconstruction.

One of the most important geometric requisites, is that the axis of rotation of the scanner has to be aligned with the center of the images. In x-ray CT, gantry based scanners use a calibration protocol to find its exact location to then compensate for the shift or skew during the backprojection. However, as in OPT the sample rotates around its axis, the location of the center of rotation can vary from one scan to another. Besides, even if the rotating stage has not changed its position, the sample holder may present small variations in shape that prevent exact repeatability of the geometry even in sequential scans. A simple and effective way to accurately estimate the center of rotation is to iteratively maximize the total variance of a reconstructed slice by trying different values for the center of rotation [47].

The use of mechanical stages to rotate the sample can produce small vibrations that affect negatively the quality of the reconstructions. Moreover, motion of in vivo samples can introduce equivalent artifacts that of the mechanical system. These perturbations can be usually modeled as small displacements and rotations and their amplitudes can be estimated from the sinogram to be further compensated in the reconstruction [24,48]. Another approach to remove jitter from vibrations or deviations from the center of rotation is to use Phase-Retrieved Tomography (PRT) [49]. This algorithm for misaligned LSFM and OPT data backprojects the autocorrelation sinogram instead of the filtered sinogram as it is inherently aligned. Then, the object can be reconstructed via a phase retrieval algorithm. The advantage of this reconstruction method is that no prior information of the misalignments is needed, neither to estimate their amplitudes explicitly.

2.3. Flow measurements

Blood flow measurements in vertebrates play an important role in angiogenesis and vasculogenesis research. OPT has been used through several implementations to obtain contrast from moving bloodstream cells, enabling the reconstruction of a 3D angiography of the specimen. Among them, flow-OPT uses a motion-analysis algorithm to process several time frames of the specimen [25]. Later, the same group introduced Optical Vector Field Tomography (OVFT), which the data using Particle Image Velocimetry to obtain label free contrast from the velocity map of blood cells in the vasculature of zebrafish [50]. Another technique to measure blood flow is laser Doppler Projection Tomography (LDPT), which extracts the flowing signal measuring time-dependent fluctuations of Doppler-shifted light due to moving scatterers. The signals from moving and non moving particles are separated in the frequency space and 3D images are obtained using FBP [51].

2.4. Considerations for sample preparation

As in most optical imaging techniques, sample preparation is crucial to minimize the refraction index mismatch between the optics and the medium. Even if immersion objectives are used, the refraction index might not be constant across all interfaces. Basic schemes to include small mismatches in the reconstruction consist on removing affected projection rays [52]. If the index of the medium and the lens are known, the deviation of the rays from the ideal geometry can be calculated and compensated for transmission OPT [53]. This work also suggests interesting corrections for background illumination uniformity and defective pixels from the CCD.

Another issue that arises from sample preparation is the homogenization of the absorption coefficient during tissue clearing. As transillumination OPT contrast relies on tissue attenuation, these protocols can hide structures of interest. This can be addressed using polarized light to detect them [54]. Acquiring tomographic data sets for different orientations of the analyzer can reveal contrast from certain structures such as oriented muscle fibers [55].

2.5. Summary

OPT has been widely used to study a large variety of biological processes such as developmental [56], in vivo vasculature [25], whole cleared organs [57] or plants structure [58]. This technique can generate high resolution three dimensional reconstructions from absorption and fluorescence contrast. Its tomographic nature provides isotropic resolution in terms of voxel size, however, the spatial resolution of the axial slices decreases radially [59]. In addition, this technique requires to rotate the sample, which is performed using mechanical stages that can lead to long acquisition times. The acquisition geometry allows to implement advanced longitudinal acquisition protocols to scan very large samples without resorting to volume stitching as in helical OPT (hOPT) [60]. Transmission OPT is a quite unique modality, as no other optical imaging technique uses absorption to image anatomical structures of microscopic and mesoscopic size samples. Unfortunately, the isotropic emission pattern of fluorescent sources and the scattering of biological tissues forces the use of very low NA objective lenses, which significantly limit the collection efficiency. When scanning large specimens in OPT, often the DOF cannot cover the entire sample. In these cases, axial scanning can be used to acquire projections with the entire sample in focus. This approach tolerates the use of objectives with higher NA, which can help to reject out of focus light and improve the quality of the reconstructions.

3. Light sheet fluorescence microscopy

LSFM is a three dimensional optical imaging technique that has spread through most of the research groups focused on the study of biological processes in large sized microscopic specimens. This recently emerged technique has evolved very rapidly due to its relative simplicity and outstanding performance in terms of spatial and temporal resolution. Light sheet microscopy supports a large variety of variants and implementations and has become an indispensable tool for in vivo and in vitro imaging in a wide range of applications.

The first time that light sheet was used for imaging took place at the beginning of the 20th century, when Siedentopf and Zsigmondy were looking for a method to enhance the resolution of their microscope. They first proposed the idea of generating a plane of light by illuminating a rectangular thin slit that, focused with a condenser lens, would result in a thin sheet of light. The optical axis of the eyepiece was mounted perpendicularly to the illumination path, this way, they could observe the scattered light by a thin section of the colloid [61]. The invention allowed Zsigmondy to observe and measure single gold particles with diameters of less than 4 nm [62]. By then, the lack of technologies to capture the images made illustrations the only way to register the results. His findings using this new microscopy technique, named Ultramicroscopy, honored him with the Nobel Prize for Chemistry in 1925. Nearly a century later in 1993, Zsigmondy's idea was used again to image biological samples for the first time ever in a technique named Orthogonal-Plane Fluorescence Optical Sectioning (OPFOS) [63]. In the early2000ŕs, Thin Light Sheet Microscope (TLSM) [64] permitted to observe microbes suspended in seawater with sharp contrast, obtaining images with very low background intensity due to the precise excitation achieved. Light sheet microscopy became popular after the publication in 2004 of a paper in Science by Huisken et al. [65], reviewing the invention and presenting it as we know it today. The technique this time was termed Selective Plane Illumination Microscopy (SPIM) and triggered a revolution in the field that has permitted to capture three dimensional images without requiring any reconstruction algorithm with high spatial and temporal resolution as never imagined before.

3.1. Setup design and considerations

The basic idea behind LSFM is to excite a fluorescent sample using a very thin sheet of light while collecting the emitted fluorescence from the orthogonal direction (see Fig. 1). If the sample is transparent enough, the camera will capture the distribution of the fluorophore in a thin section of the specimen. Then, the sample is sequentially translated towards the camera to section more slices, resulting in a 3D representation of fluorophore as a stack of images. There are two basic methods for light sheet generation (see Fig 2), known as static and dynamic light sheets, that will give different properties to the microscope. Nevertheless, all pursuit the same goal of creating a light sheet as long and thin as possible across the entire field of view (FOV).

Static light sheets are formed using a cylindrical lens to expand a gaussian beam in one axis. Then, an objective lens typically with low numerical aperture (NA) focuses the light into the field of view. This method was used by Huisken et al.[65] and is the easiest one to implement. Static light sheets often suffer from optical aberrations and have restricted efficiency delivering the excitation intensity to the sample. These limitations motivated the rise of Digitally Scanned Light Sheet Microscopy (DSLM) [66], where a virtual plane of light is generated with a gaussian beam translated along the plane of interest at high speed, typically using a set of galvanometric mirrors. Dynamic light sheets have advantageous properties due to their incoherent nature, rendering a more homogeneous excitation across the FOV due to their better energy confinement. Moreover, they are compatible with more complex scanned beam shapes or multi photon excitation [67].

The choice of optics for illumination is a determining factor of the performance of the microscope. In fact, during the design and assembly of the microscope, engineers need to find a compromise between the desired length of the FOV, given by the depth of field, and the optical sectioning power, determined by the thickness of the waist at the rear focal plane of the illumination objective. The use of low NA objectives

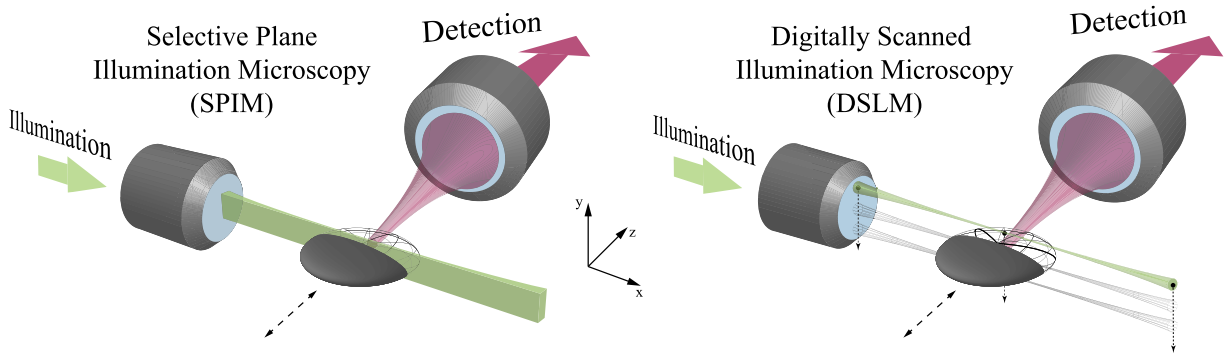

Fig. 2. SPIM excites with a thin sheet of light generated using a cylindrical lens located at the back focal plane of the objective lens. In DSLM, a gaussian beam is swept at high speed along the detection focal plane to generate a virtual light sheet.

generate long light sheets with limited waist thinness whereas high NA will lead to very thin light sheets with good optical sectioning but short FOV. Although low NA optics are preferred for light sheet generation, this decision is subject to the microscope's geometry, type of sample holder, purpose of the images and other acquisition parameters such as speed or resolution.

3.2. Advanced illumination and detection schemes

As light sheet illumination occurs in the ballistic regime of light propagation, samples that contain dense structures usually produce stripe artifacts into the images. These are caused by the interactions of the plane of light with absorbing or scattering particles while propagating in the excitation plane. The shadows and diffraction patterns formed behind these structures lead to obscured stripes in the images due to lack of excitation. This artifact is very common in LSFM, specially when using static light sheets due to their coherent nature. There are several strategies in the literature to reduce these artifacts such as pivoting the light sheet while scanning [68], using dual side illumination [69], performing multi view acquisitions [70,71] or a combination of several [72,73].

Multi view LSFM can achieve very good results but increases phototoxicity and the acquisition time. A recent work proposes a smart rotation workflow that identifies the angular positions with optimal view in terms of optical accessibility [74]. This approach reduces the dose delivered to the sample and discards those views where optical obstacles yield to poor image quality. Multi view LSFM can be also used in combination with computational techniques such as subvoxel resolution [75] to achieve very high isotropic resolutions [76].

Pivoting the light sheet or the scanning beam with a galvomirror is limited in speed by the inertia of the rotating mirrors. Despite the use of resonant mirrors has shown higher speed upper bound [68], acousto optical deflectors (AOD) demonstrated the best performance in this task [77]. In fact, this technology allows not only to pivot the light sheet, but also to generate concurrent beams with different pivot angles. The AOD splits the beam into a 0^{th} undeviated beam and a 1^{st} order deflected beam. The use of multiple frequencies allows to illuminate with several pivot angles at the same time, however, this comes at the cost of splitting the power among the simultaneous beams.

Instead of using a multi view or a pivoting method, the use of a convectional incoherent LED sources can suppress shadowing artifacts [78]. In order to obtain volumetric information, a spatial modulator structures the illumination light along the detection direction and the acquired encoded data needs to be reconstructed to obtain the final volume. This approach not only eliminates stripe and speckle derived artifacts, but can also reduce the cost of the system.

Recently, the use of a line diffuser was suggested as an approach to homogenize the excitation and reduce the stripe artifacts either in DSLM and SPIM [79]. In the study, no variation in the axial profile of the light sheet was noticed and, as in other stripe reduction methods, this approach is not compatible with confocal slit detection.

A more sophisticated technique for stripe removal is to use multi modality imaging. Transillumination OPT renders an absorption map of the sample that can be used to correct the fluorescence images [80]. In light sheet microscopy, OPT images can not only compensate the heterogeneous illumination to reduce stripe artifacts but also the attenuation of the emitted fluorescence while propagating towards the detection axis [81].

Gaussian beams, although offering good balance between simplicity in the implementation and optical performance, are prone to create stripe artifacts if the medium presents inhomogeneities and have fast divergence if a very thin waist is required. Light sheet engineering aims to overcome these limitations with other kind of beams that are more robust to scatterers, have larger FOV and better energy confinement across it. Bessel beams are one of the most common ones due to their easy generation and self healing properties [82], offering stable optical sectioning for significantly longer fields of view than Gaussian beams [83,84]. These properties make them suitable to image large and heterogeneous samples with very homogeneous excitation.

Side illumination is the main disadvantage of Bessel beams, which excites out of plane fluorescence that lowers the signal to noise ratio and thus the contrast of the images [82]. This effect is more prevalent in single photon excitation, where the lateral and axial resolution can be even worse than with gaussian beams [85]. Nevertheless, the higher energy confinement within the main lobe of bessel beams make them very efficient for multi photon excitation. Its non linear response prevents side lobes from generating any out of plane signal [84,86]. In fact, a recent work has demonstrated for the first time 3 photon excitation in light sheet microscopy [87] where again, bessel beams were able to excite a larger field of view. Three photon light sheet shown to provide better contrast than 2 photon in deep tissue at depths of at least 450μm

In order to reduce the downsides, image contrast with bessel beam single photon LSFM can be improved through confocal line detection, an acquisition method for DSLM in which the camera rolling shutter is synchronized with the scanning to reject photons that arrive to the detector out of an activated line of pixels as shown in Fig. 4) [82]. A recent work presented an alternative method to minimize side lobes in bessel beam illumination by rescanning the sample with a complementary zero order bessel beam that excites only out of focus fluorescence. Then, both images are subtracted to improve the axial resolution from 1.68 μm to 1.07 μm in a field of view of 300 x 200 x 200 μm[88].

Another type of engineered scanned illumination are Airy beams, which can be generated by a cubic phase mask. Their constant profile in propagation demonstrated to excite ten and four times longer FOVs than gaussian and bessel beams [89], respectively. In order to recover near-

diffraction limited resolution, imaging with airy beams requires further image convolution to suppress the fluorescence from the side lobes and artifacts due to their curved profile. A more complex approach is the use of Lattice light sheets, which are built upon a coherent addition of non diffracting Bessel beams. The resulting 2D optical lattice can conform a plane of light using a dithered scanning mode or structured illumination, the latter enabling super-resolution imaging [90]. Although lattice light sheets exhibit extremely low photobleaching and minimal phototoxicity with axial resolutions in dithered mode of 370 nm, their range of applications is limited as they depend strongly on coherent interactions, thus, the specimen thickness must be kept below 20μm to 100μm.

Engineered beams require complex optical setups and rather expensive components such as spatial light modulators (SLM). Furthermore, depending on the choice of implementation, a setup can be exclusive for a certain kind of beam. Light Field Synthesis [91] is an optical theorem to generate any scanned or dithered light sheet using a universal method. The time averaged light distribution of the desired beam is created by a line scanning a pupil in the fourier domain located at the back focal plane of the illumination objective. In addition, this technique can substantially reduce the cost of the illumination arm as no SLM is needed.

Each of these beam shapes has its own strengths and weaknesses and in general it is difficult to give a short answer about which one gives better performance or is more suitable for a certain application. There are some works aiming to establish protocols to select and optimize the excitation light based on the desired spatial resolution, sample size, desired FOV and axial resolution or requirements of the sample [92]. A recent study suggests that there is a strong trade off between optical sectioning performance and axial resolution, being the choice of light sheet thickness a key factor [93]. Very thin engineered light sheets often carry stronger side lobes that lead to a reduction of the contrast of the images. Even though deconvolution can revert the effects of side illumination, there are limitations to the amount of background it can remove and thus the recommendation is to minimize side lobes as possible. In general, Gaussian beams are the best choice to maximize contrast and FOV except for multi photon excitation, where Bessel beams give the best optical sectioning and constant propagation profile.

An alternative way to excite deeper tissue is to image with wavelengths that present less scattering in biological tissue. Near infrared light meets this property [94], in fact, this is one of the reasons that explain the depth of penetration of multi photon excitation. Moreover, autofluorescence is nearly nonexistent at these wavelengths, which improves the signal to noise ratio. Scattering in the near infrared is specially low in the second window, which comprises the range between 1300 nm and 1700 nm [95]. A recent work has investigated light sheet in this window, using excitation and emission wavelengths of 1320 nm and 1720 nm, respectively. The images shown axial resolutions of 7–17 μm up to 750 μm depth in living mouse brain tissue through the intact skull [96].

The detection in standard light sheet microscopes has rather less complexity than the illumination and is usually composed by an objective lens, an emission filter, a tube lens and a camera. The NA of the detection objective is decisive to achieve good lateral resolution. The DOF of the objective lens must be chosen according to the thickness of the light sheet in order to cover its axial whole thickness, otherwise out of focus excited photons reaching the camera will degrade image quality, introducing background intensity and blurriness. The working distance of the objective lens must be carefully taken into account when aiming to image thick samples as focusing at the deepest planes requires to place it very close to the sample's surface [97].

Scanning large samples in LSFM with gaussian beams comes at the cost of sacrificing axial resolution. As mentioned earlier, to have large FOVs the divergence of the beam cone must be minimized using very low NAs, which render gaussian profiles with thick waists. An approach to extend the DOF of a beam it is to generate through incoherent addition a constant thickness light sheet by sweeping the waist along the propagation direction. This can be made using at high speed with an acousto-optical tunable lens [98] or a remote focusing objective [99] (see Fig. 3). The latter, combined with confocal line detection in Axially Swept Light Sheet Microscopy (ASLM) [99] (see Fig. 3), can achieve isotropic resolution of 390 nm over hundreds of μm and up to 290 nm in cleared-tissue ASLM (ctASLM) [100]. In combination with dual side illumination, multi view acquisitions with extended DOF can also be performed [101]. Recently, very large FOVs were demonstrated with a resolution of 1.7μm over 3.3 mm and speeds of up to 20 frames per second by oscillating the illumination objective with a voice coil motor (VCM) in confocal DSLM [102] (see Fig. 4).

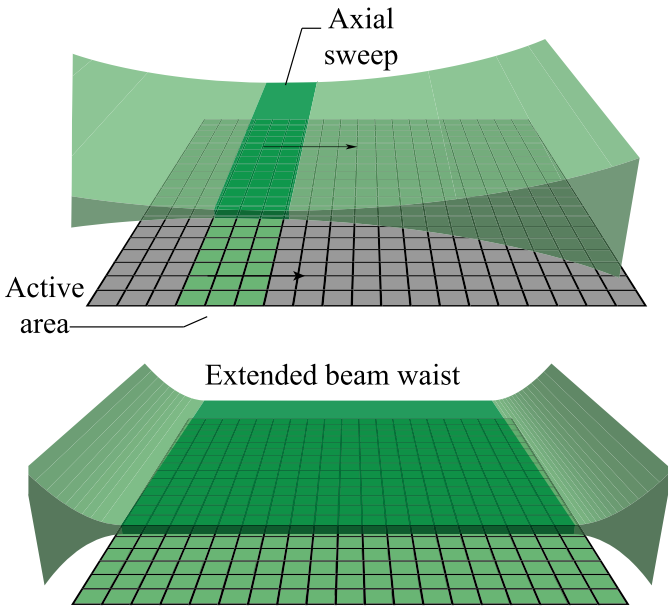

Fig. 3. Axially swept light sheet (ASLM) achieves uniform averaged sheet waist across the FOV (bottom) through axial shifting of the light sheet combined with the camera rolling shutter [99].

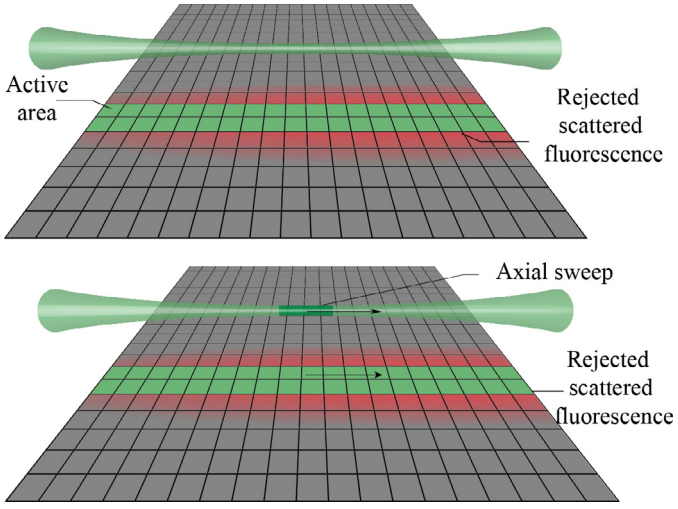

Fig. 4. Confocal detection in lightsheet (top) helps to reject scattered light to reduce the background intensity [101,103]. Together with axial sweeping allows to improve optical sectioning [102].

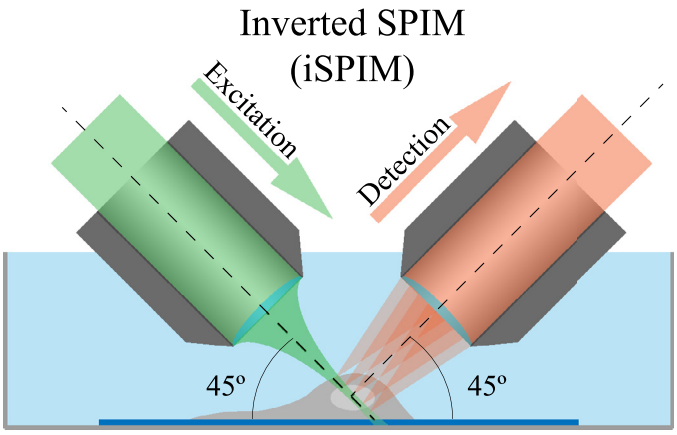

Fig. 5. Arrangement of lenses in the inverted configuration. Two immersion lenses illuminate and collect at 45° respect to the coverslip surface.

A step beyond axially swept light sheets are tailored bessel beams. This technique tunes dynamically the position and the length of the focus within the FOV. Together with the camera rolling shutter (see Fig. 4) achieves an increase in the contrast of up to 70% [103], scanning up to 200 different beams per frame. In addition, photobleaching is reduced and by variating the intensity of the laser the variations in the fluorophore concentration or in the absorption of the sample can be compensated. This method is particularly interesting to scan samples with complicated and asymetric shapes such as Arabidopsis. Another interesting way of increasing the penetration of propagation invariant beams is to tailor its longitudinal envelope by weighting the complex amplitudes of the different wave vectors of the phase mask. This allows to compensate for the attenuation of the sample and to achieve uniform excitation and greater contrast in deep tissue layers [104].

Speeding up light sheet acquisitions has strict limitations if the translation of the sample or the system is performed with mechanical stages. Instead, an electrically tunable lens (ETL) can be used to shift the detection focal plane and a set of galvomirrors to tranlsate the lightsheet [105]. Even faster speeds can be reached if the excitation plane is shifted with an acousto-optic scanner and an acoustic tunable lens (TAG) is used to refocus [106]. Any of these methods achieve speeds not comparable with mechanical translation and avoid any kind of undesired vibrations.

3.3. Advances in light sheet variants

The classical LSFM setup has an orthogonal arrangement of the illumination and detection objectives, both lying in a horizontal plane. This configuration was originally designed to image samples that can be embedded in agarose and mounted in Fluorinated Ethylene Propylene (FEP) tubes. Nevertheless, this layout limits the compatibility of the technique with other traditional sample holders, such as glass coverslips or culture dishes, due to the presence of the illumination objective lens at the same plane as the sample. This geometry impedes the use of short working distance lenses, with the additional risk of colliding with the holder.

These constraints motivated scientists to modify the standard light sheet configuration to accommodate alternative sample holders. Several alternative architectures can be found in the literature, being the most common the inverted SPIM (iSPIM), the open-top SPIM and the Oblique Plane light sheet microscopy (OPM).

3.3.1. Inverted light sheet microscopy

iSPIM is the result of moving the detection objective to the vertical axis, as in an inverted microscope and rotating the whole arrangement 45 degrees [107,108] (see Fig. 5). An advantage of this configuration is that it can be installed in the pillar of a standard microscope to image cell cultures or small embryos. Further versions are capable of illuminating and detecting from both objective lenses as in Dual-Illumination iSPIM [109,110]. In order to avoid spherical aberrations, this microscope uses water immersion objectives but unfortunately, due to their close and orthogonal arrangement, long working distances are needed and thus the choice of NA is limited for iSPIM. Moreover, since the sample stays stationary the area that can be scanned is very restricted.

A peculiar variation of the inverted configuration is the πSPIM [111], which uses a non-orthogonal arrangement of the lenses. In this system an oil immersion illumination objective lies beneath the sample, keeping the detection in an upright position but tilted at a certain angle. An oblique light sheet is generated by passing an off-center beam through the illumination lens, accommodating its angle to illuminate perpendicularly to the tilted detection axis. This configuration allows to position the lenses very close to the sample, however its use is restricted to study cell populations prepared in culture dishes.

Exploiting the fact that LSFM ideally requires from larger NAs in the detection than the illumination side, Light Sheet Theta Microscopy (LSTM) [112]) proposes the use of 2 non-orthogonal illumination arms with a widefield view high NA detection objective in between. The longer working distance and tilted position of the illumination objectives allows to place the detection lens very close to the sample. Moreover, the illumination arms are coordinated with the camera rolling shutter to perform line scanning at the intersection of the light sheets. The beam waists are translated along their propagation axis using an ETL and across the FOV with a galvomirror, always intersecting at their thinner part. The angle between the detection and the illumination objectives is tuned to minimize the propagation distance of the beams through the sample and thus maximize the axial resolution.

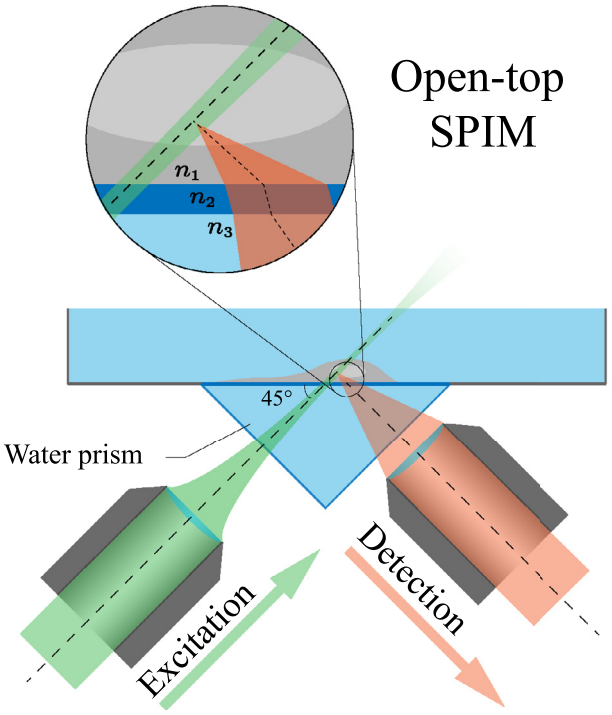

Fig. 6. In open-top light sheet microscopy, the objectives are located beneath the sample, leaving the sample accesible from the top. In this configuration, index refraction matching between the air, water and glass interface is crucial to avoid aberration.

3.3.2. Open-top light sheet microscopy

The Open-top light sheet [113] is a SPIM variant in which all the optical elements are placed beneath the sample in the same arrangement as in iSPIM (see Fig. 6). However, in this configuration there

is direct access to the specimen holder from the top of the system, facilitating the manipulation of microfluidic chips or large multi-well plates. Furthermore, objective lenses are not dipped into the sample's medium, eliminating the risk of inter-specimen contamination or damaging the objectives with corrosive organic-solvents from some clearing agents.

Since light now has to go through a coverslip arranged at 45° from the illumination and detection paths, images are very prone to suffer from large aberrations (see Fig. 6). This problem can be overcome by installing a water-filled crystal prism underneath the sample so its faces are lie perpendicular to the optical axes of the air objective lenses. Despite the index mismatching problem being apparently solved, light crossing the 45° oriented slide still introduces astigmatic aberrations. These are compensated by adding a weak cylindrical lens after the tube lens in the detection line. In the illumination side a slit reduces the NA of the objective, extending the length of the light sheet and suppressing the aberrations.

The open-top configuration described above can only mount relatively low NA optics due to high order aberrations from the coverslip interface. An adaptive optics module was suggested to compensate for them [117] however, other works have rather chosen to refine the design, replacing the water prism for a hemispherical solid immersion lens (SIL) [115] (see Fig. 7). This approach has several advantages over the water prism. As the SIL has a curved surface at its bottom that approximates to the wave-front curvature, the air-medium interface is well matched. Moreover, the flat surface at the top matches the index of refraction of the slide. The addition of an oil drop between the SIL and the slide allows the latter to be translated without friction to scan large areas. Since the SIL must be placed in contact with the surface of the sample holder and its alignment with the objectives is critical for the system's performance, there is no z axis displacement of the sample and hence this configuration is only suitable for 2D imaging or for very thin samples.

Recent advances have enabled to scan samples in 3D using an open-top configuration. Based on the idea of the water prism, multi-immersion open-top light sheet [114] (see Fig. 7) introduces a more sophisticated index matching chamber beneath the glass slide. This chamber contains an interchangeable immersion medium to accommodate to the exact index of refraction of the sample or clearing protocol. The excitation light is delivered through an air objective coupled to an immersion lens interface of the chamber that accounts for the medium to air index of refraction change. However, the detection is performed through a multi-immersion objective lens that can be inserted into the chamber to allow shorter working distance lenses. The top slide can be also exchanged to use the most suitable glass material according to the refracting index of the sample, determined by the clearing protocol. This design is less restricted to scan thick specimens than previous open-top microscopes, being capable of imaging at depths of up to 0.5 cm in an area of up to 10x10 cm with sub-micron resolution. However, the use of mechanical stages to translate the sample prevents it from being using to image living specimens.

Finally, a hybrid approach between water prisms and SIL was recently published. Named as solid immersion meniscus lens (SIMlens) [116] (see Fig. 7), consists of a custom prism immersion bath with a meniscus lens window for each optical axis (illumination and detection). This design allows to mount any air objective since the meniscus lens, if chosen carefully, performs the wavefront match with the immersion medium. Besides, the use of air objectives reduces the cost of the system and permits to switch them easily. In contrast to the SIL version, the sample plate can be freely displaced in the z axis, enabling 3D imaging of several mm depth.

Open-top configurations are evolving quickly and their advances so far have been focused on carefully refine the index matching of the whole optical flow to minimize aberrations, and increase the flexibility of the system to accommodate larger and thicker samples.

3.3.3. Single objective light sheet microscopy

Owing to the orthogonal arrangement of the optical paths in LSFM, the use of two objective lenses is the most straight forward implementation. However, this can be problematic in some applications since forces the use of long working distance objectives, complicates the alignment of the system and has a large footprint that can limit the compatibility with other instruments [118,119]. Light sheet through a single objective lens couples the illumination and detection through the same optical axis, allowing to place the objective very close to the sample and increasing the range of NA. Illuminating from an orthogonal direction in this configuration is very challenging but it can be achieved in a simple way with Single Objective SPIM (soSPIM) [120]. Here, micromirrored cavities at the sample's well are used to reflect an off axis laser beam passed through the detection lens. soSPIM can be applied to any inverted microscope but, as other mirror based approaches [121], need from additional hardware and are restricted to reduced size samples.

3.3.4. Oblique plane light sheet microscopy

Oblique plane microscopy (OPM) [122] differs from the rest of LSFM configurations for being a real standalone single objective LS microscope. Unlike most light sheet variants, the illumination is delivered with an off axis beam passed through the detection objective that creates an oblique light sheet geometry. Due to the resulting non orthogonal arrangement, the excitation is not fully confocal to the detection plane anymore and thus part of the light is captured out of focus. This issue has be compensated by adding a reimaging system in the detection line [123] that (see Fig. 8). The remote imaging module consists of a pair of opposed objective lenses tilted according to the obliquity of the light sheet. A limitation of this technique is that the coupling of the NAs cause that part of the cone of light from the secondary objective is not covered by the tertiary, yielding a non isotropic PSF at the imaging plane and cropping the original NA of the first lens. Moreover, higher tilting angles will increase the resolution anisotropy and require from wider apertures [124]. In this case, using immersion objective lenses can help to 'compress' the k-vectors and reduce the resolution loss.

Recent works have put strong efforts to reduce the resolution loss in OPM. Oblique epi-illumination SPIM (eSPIM) [125] proposes the use of a pair of index mismatched objective lenses at the remote focusing module to compress the angle of the refocused light. This is achieved by placing an air to water interface between the secondary and the tertiary objective lenses that ensure full coverage of the entire cone of light. This modification allowed to keep the front objective's NA through the entire optical path of the microscope. Another idea followed in single-molecule oblique-plane microscopy (obSTORM) [126] is to place a mirror at the focal plane of the second objective to reuse it as a third objective. The mirror is slightly tilted to allow to refocus the oblique image. Despite this design simplifies the optical setup, the use of a single objective remote focusing module requires from the use of a beamsplitter that added to the mirror losses by reflection drops the light efficiency to 25% from that of a conventional STORM microscope. Redesigning the third objective can allow to achieve full numerical aperture of the primary objective coverage. In this case this lens incorporates a glass tip that enables zero working distance imaging in the remote imaging module [127] to cover the entire cone of light.

Imaging with low NA objective lenses to cover larger fields of view in OPM is technically very challenging since narrow collection angles increase the tilt between the objectives in the re-imaging module and thus the aperture mismatch. In the worst cases, the tertiary objective wouldn't even collect the light from the secondary. However, a reflective blazed diffraction grating placed between the re-imaging objective lenses can redirect the light in almost perpendicular direction respect to the secondary lens optical axis [128]. The co-alignment of the grating with the oblique plane enables optimal re-imaging using low NA lenses. This design demonstrated OPM in large volumes of up to several mm at high speed using lenses of NA 0.28.

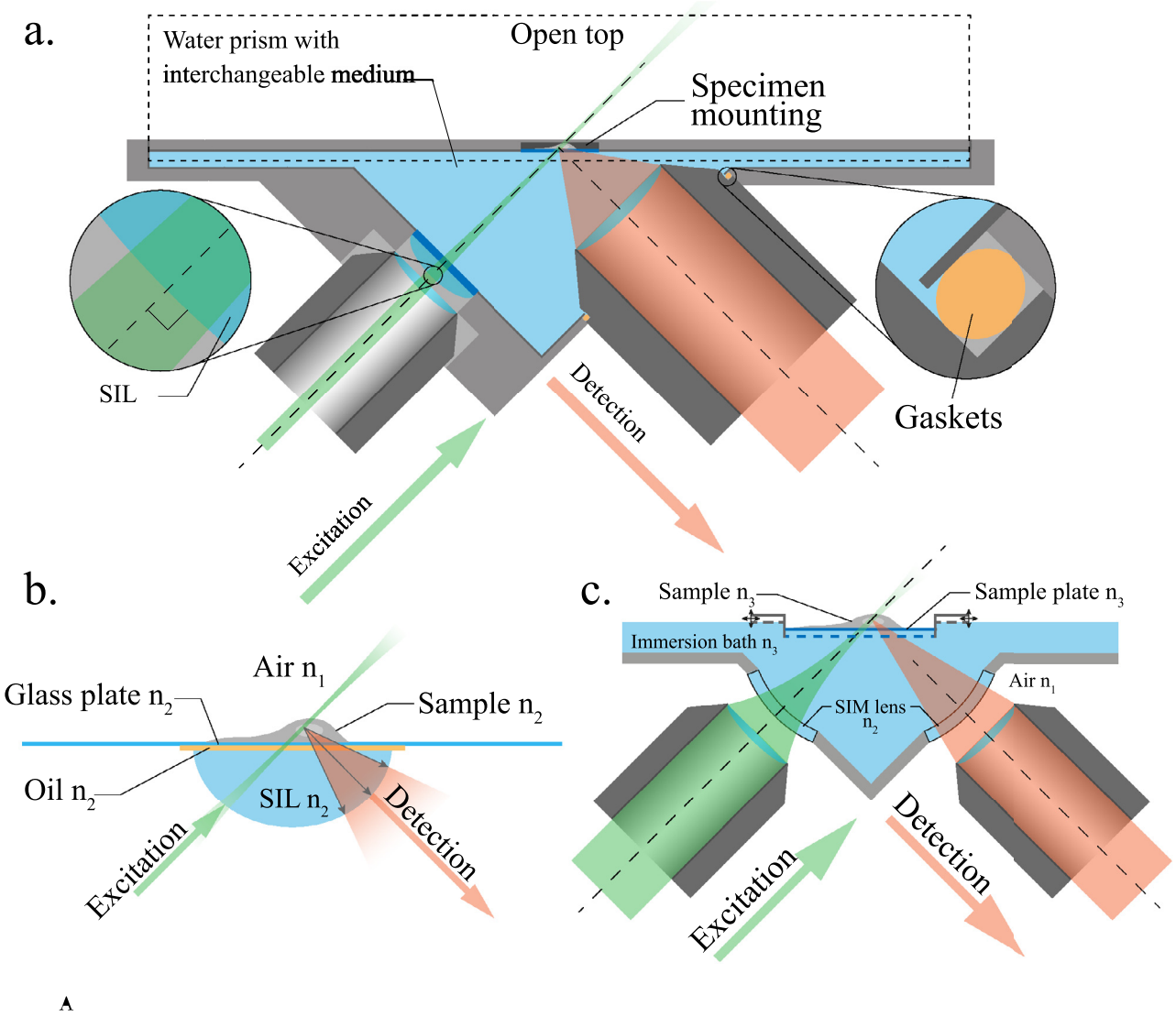

Fig. 7. Approaches to improve the index matching problem in open-top light sheet microscopes. In a., a multi-immersion objective is inserted into an interchangeable immersion medium chamber [114]. Solid immersion lenses can perform waveform matching given their large curvature. In b. a hemispherical lens is attached under the slide [115], whereas in c. two meniscus lenses are embed in the walls of the prism [116].

OPM systems originally relied on mechanical stages to translate the sample through the detection focal plane and across the limited field of view [122]. Mounting the second objective in a piezo-electric actuator allowed control the axial position of the light sheet and tilted observation plane in the sample [129] however, mechanical translation has shown to be slow and limits the scanning speed [130]. Similarly to confocal theta microscopy [131], in Swept Confocally-Aligned Planar Excitation (SCAPE) microscopy [132] a rotating polygon mirror mounted in a galvanometer motor was used to scan the light sheet. Simultaneously, the captured fluorescence is de-scanned by reflecting it back into an adjacent face of the polygon. This creates a stationary oblique image plane in the remote focusing module regardless of the position of the light sheet. With this method very high acquisition speeds can be reached, capturing up to 24 volumes per second with very large fields of view of up to 600 x 1000 x 550 μm.

Though SCAPE is a very high performance system, using a polygonal mirror produces tilt-variant scanning planes, requiring from further postprocessing to rearrange the data. Instead, other systems have developed tilt invariant scanning methods. In Scanned Oblique Plane illumination (SOPi) [133], a scanning mirror inserted in the Fourier plane of a 4f system allows to scan the light sheet along the sample at high seed without changing the tilt angle. A second galvomirror enables to scan in DSLM mode to perform 2-photon excitation. Together with rolling shutter confocal detection the resolution of the system is improved at the cost of reducing the speed. The relatively low NA of this system limits the 2 photon excitiation efficiency, however using Bessel beam excitation could significantly increase its performance [134].

During the preparation of this review, the SCAPE team presented their renovated SCAPE 2.0 [135], in which the polygonal mirror has been substituted for a large aperture galvanometric mirror. As in other OPM setups, this component carries out the scanning of the light-sheet and descanning of the fluorescence, generating a static intermediate image plane that is re-imaged by the remote module to obtain a sharp in focus image. The SCAPE 2.0 has also incorporated a

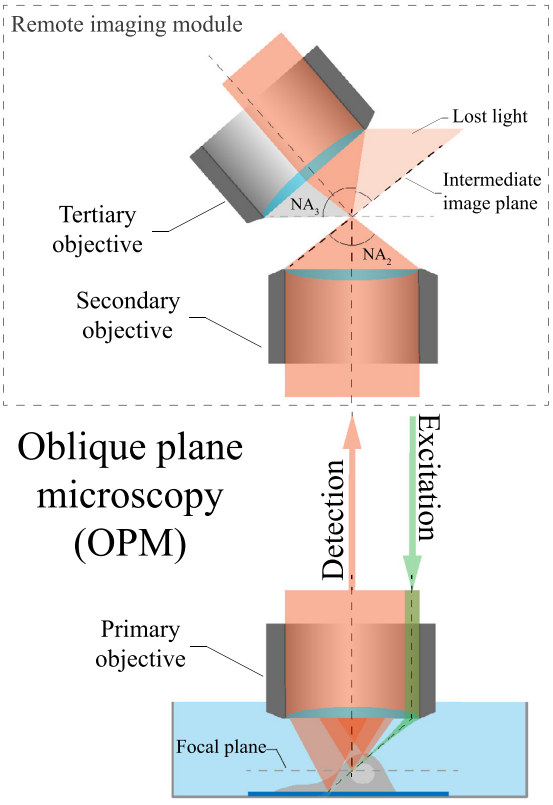

Fig. 8. Diagram of an Oblique plane microscope (OPM). The fluorescence excited in an oblique plane needs to be refocused with a the remote imaging module. Depending on the inclination of the illumination plane and the NA of the objective lenses, part of the light might be lost in the intermediate image plane.

high speed intensified camera that provides unprecedented acquisition speeds of up to 300 VPS, capturing near-isotropic freely moving *c. elegans* and real time blood flow in the beating zebrafish heart. In addition, the primary objective lens has been mounted in a rotating mirrored cage to image samples from top-down, inverted configuration or even side-facing.

Although OPM systems can shift the plane of light across the sample to obtain 3D volumes, the high NA conditions the working distance and limits the size of the FOV. Recently, thank to the development of tilt invariant scanning geometries [133], large volumes of several mm length could be imaged by stitching volumes in postprocessing [136]. there is a high NA single objective for OPM systems that delivers full numerical aperture of the primary objective through a glass tip that enables zero working distance imaging in the remote imaging module [127]. Also, the same group proposes a remote refocusing module for high-speed high-resolution microscopy. In both projects, there is a repository with all the necessary documentation be replicated.

3.4. Sample manipulation in light sheet microscopy

Light sheet microscopes relies on the transparency of the samples to acquire high resolution images. Specimens have usually very reduced size or have been treated to be transparent [137,138]. On the other size, for non living samples usually optical clearing protocols are used to have a homogeneous refraction index in the samples and minimize scattering [139,140]. However, careful sample preparation is a key step to ensure stability, avoid sample motions or reduce the aberrations during the imaging process [141]. Recent publications have presented some innovative ideas for sample holders and methods to control the position and orientation of the specimen.

Rotating the sample in multi view LSFM can present difficulties, especially if its orientation needs to be kept during the whole experiment [142]. The use of a magnetic field [143] has been proposed in this work to manipulating small agarose spheres with embedded magnetic beads. The forces applied must be carefully controlled to avoid deformations or damages to the sphere due to displacements of the beads. The method was applied to image zebrafish embryos, larvae, mouse embryos and shrimps. High throughput imaging could be greatly benefited from this technique as there is often no control over sample orientation [144].

In some applications, embedding samples in agarose can have negative effects for their development, growth or diffusion of drugs and fluids [145]. Thus, some applications can benefit from non contact confinement of samples during the imaging process. This can be achieved using optical traps for cell sized specimens [146]. In fact, conventional microscopes equipped with optical tweezers can be used for light sheet microscopy if a small cantilever mirror is installed at the sample chamber [147]. This setup enables optical manipulation using gaussian and bessel beams with line confocal detection to achieve high contrast imaging.

Since optical traps can only apply forces of up to several pN, larger samples like zebrafish larvae can be manipulated with acoustic gradient force traps. With this technique, the dynamic response of the specimen can be studied without affecting the perfusion rate or drug delivery [148].

In a recent publication, light sheet microscopy was proposed as a technique to monitor cell and tissue manipulations such as sub-cellular ablations or tissue cauterization [149]. This setup combines a multi view SPIM with an IR femtosecond based photo-manipulation module to visualize the sample in 3D with high spatio-temporal resolution.

4. The open microscopy community

Acquiring a state-of-the-art microscope requires a large investment for the hardware and often to purchase additional modules or postprocessing software separately. Biologists and end users are often interested in commercial systems since they usually include technical support and usage training. However, since the commercialization of LSFM and OPT technologies by the main microscopy manufacturers took several years, interdisciplinary teams have built their imaging systems at the lab [150]. In fact, nowadays the community of microscopy developers is still dominated by custom made equipment [151].

Home built microscopes have several advantages over commercial systems. As cutting edge features are usually developed first in academia, it is easier for engineers to work in custom setups that have not been packed in a compact device or have closed software and proprietary tools. This gives more flexibility to make modifications and build new configurations [151]. Besides, the budget for custom built microscopes can get substantially reduced, allowing to mount higher end components.

Despite all these advantages, building your own microscope requires highly skilled personnel, technical background and some previous expertise. Therefore, even if advice from the literature is followed [8], designing a system from scratch can be time consuming and a waste of resources. Fortunately, the light sheet and OPT community has a strong movement of open hardware projects. These are microscopes that have all the technical details available for the community, so researchers can easily build their own versions, customize them and publish their results. Some of them have been around for a while and quite extended but others have just landed and carry the latest advances in the technique.

The most popular open light sheet initiatives are OpenSPIM [152] and OpenSpinMicroscopy [23]. OpenSPIM [152] is self defined as an open source SPIM platform and their website contains full instructions and partlist to build your own system. Additionally, it uses Open Source software to control the device, programmed for μManager

[153,154] and Fiji [155]. Components are affordable, even 3D printable in some cases, and has extended its features to perform multi view deconvolution and brightfield illumination. Also, a new toolbox for beam shaping compatible with the OpenSPIM platform was released recently. Structured SPIM (SSPIM) [156] allows to generate digital patterns to illuminate with the most common light sheets using a SLM. Similarly, OpenSpinMicroscopy [23] is also an open source platform that offers a variety of light sheet systems that implement SPIM, DSLM and OPT. The acquisition is controled by Arduino and has additional extension modules for microfluidics, dual side illumination and confocal slit detection. Within the framework of the OpenSpinMicroscopy platform, SPIM-fluid proposes a system designed to acquire automatized 3D high-throughput images of cell cultures and small organisms. Sample loading is carried out through a FEP tube and a pump which simplifies its manipulation and saves a significant amount of time [157].

Inspired by the open-microscopy projects described above, the mesoscale selective plane-illumination microscopy initiative (MesoSPIM) [158] was recently released. This modular state-of-the-art light sheet microscope implements multi view acquisition, DSLM and ASLM with an ETL and can image large volumes with high resolution. Sample handling is quite flexible, allowing to mount samples in FEP tubes or cuvettes with a magnetic quick exchanging system.

SPIM has also an educational purposed project called EduSPIM [159]. The control software has a very simplified user interface, optimized for college and school projects or research groups looking for a cheap and easy to use microscope. All the technical details and instruction to build one are available as supplementary materials in the publication.

There also open OPT specific project such as OptiJ [24], a low cost system that comes with ImageJ plugin for reconstruction and preprocessing of OPT acquisition. It can run in GPU and has interesting features such as sinogram dynamic offset correction.

Upgrading a light sheet system for a certain task or application usually requires large degree of expertise and skills, plus some theoretical background. The AutoPilot framework [160] is a tool for spatial resolution optimization and signal strengthening for adaptive light sheet microscopy. It provides from hardware and software modules to add, configure and fine tune adaptive imaging capability to a light sheet microscope. Despite this package is optimized for the SiMView system[72], it can be applied to any existing system. SiMView documentation, designs, and part list are available on request.

As no non-commercial deconvolution tools for LSFM yet exist, a recent work proposed an open source software for this task that makes use of an computed PSF model [161]. The code and compiled binaries can be downloaded for free and is optimized to run in multiple CPU or GPU acceleration.

On the hardware side, there are a few open source components that implement advanced capabilities in light sheet microscopes. In particular, the high NA single objective for OPM systems [127] and the remote refocusing module for high-speed high-resolution microscopy [162], both proposed by the same group, are two examples of open hardware in which a repository shared at the lab's site contains all the necessary documentation to be replicated.

Finally, computational simulations can also play a key role in the development of light sheet microscopy systems. For this task, Biobeam [163] offers an open-source platform to reproduce most of the optical phenomena that occur in a light sheet microscope such as diffraction artifacts, all kind of aberrations or the image formation process. The simulation engine uses a GPU implementation of the beam propagation method and given its modular architecture, it can be adapted to any kind of light sheet microscopy architecture. Based on the Monte Carlo method for light propagation [164], Holistic Monte-Carlo optical modelling offers a simulation environment to recreate complete imaging systems of arbitrary complexity. This software uses Monte Carlo propagation to recreate physical phenomena in the medium combined with Zemax to generate realistic microscopy images.

5. LSFM and OPT multimodal imaging

OPT and LSFM have often been compared seeking for differences in the performance of one over the other [165]. In fluorescence mode, it is clear that LSFM outperforms OPT in resolution due to its optical sectioning capacity, but also in acquisition speed and phototoxicity. However, transmission OPT and LSFM have demonstrated to be complementary imaging modalities since they couple anatomic and structural information with functional and tissue specific. LSFM despite its high resolution and superior image quality can only retrieve anatomic data while measuring autofluorescence but, unfortunately, this mode is rather unspecific and there is poor control over which structures present this property [166]. For this reason, OPT can be used as a very reliable source of reference anatomical information given its absorption based contrast [81,167].

The technological gap between OPT and SPIM has been filled by OPT-SPIM combined systems, capable of acquiring the two modalities in the same setup [23,26]. OPT can be implemented in most of the standard configuration light sheet microscopes, furthermore, given their modular architecture, OPT capabilities can be added to an existing light sheet system with minor modifications [166].

For these reasons, we strongly believe that future advances should go towards combining the best features of each of these modalities rather than forcing researchers to choose one against the other.

6. Conclusions and future perspectives

Optical Projection Tomography and Lightsheet Fluorescence Microscopy started less than two decades ago and nowadays are the best two optical microscopy techniques to image large samples in fluorescence or absorption. Although the image quality rendered by both techniques depends largely on the amount of scattering present in the tissue, the large variety of configurations, processing algorithms and sample preparation techniques developed in the last decades lead to significant improvements in the robustness, flexibility and performance of these two techniques.

OPT had a very strong impact during its first decade of development, however its use in fluorescence mode has progressively been replaced by the latest light sheet methods, capable of imaging faster, with less fotobleaching and better image quality. Transmission OPT is still a valuable technique since there is no other imaging method measuring the three dimensional distribution of the absorption, which has shown to be very convenient to complement light sheet images [81,166].

The evolution of light sheet microscopy has been much wider and diverse than OPT, with tons of new systems and configurations that can even overwhelm the people starting with this technique. Furthermore, each new system usually carries its own name, leading to a vast variety of different nomenclatures for configurations that can be classified under the same category.

During the preparation of this review, we saw the greatest advances towards single objective light sheet and open top configurations. Single objective light sheet is implemented as oblique plane microscopy and is a revolutionary configuration that changes radically the light sheet microscope layout. Despite its limited field of view, implementations like SCAPE 2.0 have demonstrated the large margin of improvement that can be still achieved in this technique by incorporating the latest detection technology an a revised optical scanning system [135]. The latest works in open top light sheet are breaking its limitations by achieving nearly perfect index matching among the multiple interfaces that this configuration presents and enabling scanning samples in the z axis[116].

Light sheet is also walking towards more flexible systems in the illumination side, capable of exciting with any kind of scanned beam without changing the setup [91] or adapting the properties of the illumination dynamically [103].

The exploration of new imaging windows is also a good step towards scanning larger samples with equivalent image quality [96].

This illumination has already shown potential in other imaging techniques[168,169], thus OPT can also get greatly benefited both in transmission and in fluorescence.

To conclude, it is also worth to mention the importance of the new open hardware systems that incorporate the latest advances, improve the accessibility to the technique and promote reproducible research [158].

Declaration of Competing Interest

1. Conflict of Interest

Potential conflict of interest exists:

We wish to draw the attention of the Editor to the following facts, which may be considered as potential conflicts of interest, and to significant financial contributions to this work:

The nature of potential conflict of interest is described below:

No conflict of interest exists. We wish to confirm that there are no known conflicts of interest associated with this publication and there has been no significant financial support for this work that could have influenced its outcome.

2. Funding Funding was received for this work.

All of the sources of funding for the work described in this publication are acknowledged below:

This work has received funding from the European Union's Horizon 2020 research and innovation programme under grant agreement No 801,347 and the Spanish Ministry of Economy and Competitiveness (MINECO) Grant FIS2016-77892-R. 3. Intellectual Property

We confirm that we have given due consideration to the protection of intellectual property associated with this work and that there are no impediments to publication, including the timing of publication, with respect to intellectual property. In so doing we confirm that we have followed the regulations of our institutions concerning intellectual property. 4. Research Ethics

We further confirm that any aspect of the work covered in this manuscript that has involved human patients has been conducted with the ethical approval of all relevant bodies and that such approvals are acknowledged within the manuscript.

IRB approval was obtained (required for studies and series of 3 or more cases)

Written consent to publish potentially identifying information, such as details or the case and photographs, was obtained from the patient(s) or their legal guardian(s).

5. Authorship

The International Committee of Medical Journal Editors (ICMJE) recommends that authorship be based on the following four criteria:

1. Substantial contributions to the conception or design of the work; or the acquisition, analysis, or interpretation of data for the work; AND

2. Drafting the work or revising it critically for important intellectual content; AND

3. Final approval of the version to be published; AND

4. Agreement to be accountable for all aspects of the work in ensuring that questions related to the accuracy or integrity of any part of the work are appropriately investigated and resolved.

All those designated as authors should meet all four criteria for authorship, and all who meet the four criteria should be identified as authors. For more information on authorship, please see http://www.icmje.org/recommendations/browse/roles-and-responsibilities/defining-the-role-of-authors-and-contributors.html#two. All listed authors meet the ICMJE criteria. We attest that all authors contributed significantly to the creation of this manuscript, each having fulfilled criteria as established by the ICMJE.

We confirm that the manuscript has been read and approved by all named authors.

We confirm that the order of authors listed in the manuscript has been approved by all named authors.

Acknowledgments

JR and AMV acknowledge funding from EU H2020 FET Open project SENSITIVE, ID 801347 and Spanish Ministry of Economy and Competitiveness (MINECO) Grant FIS2016-77892-R.

Supplementary material

Supplementary material associated with this article can be found, in the online version, at 10.1016/j.optlaseng.2020.106191.

References

[1] Pawley JB. Handbook Of Biological Confocal Microscopy. Boston, MA: Springer US; 2006. 10.1007/978-0-387-45524-2
[2] Ntziachristos V. Going deeper than microscopy: the optical imaging frontier in biology. Nat Method 2010;7:603–14. doi:10.1038/nmeth.1483.
[3] Ripoll J. Principles of Diffuse Light Propagation: Light Propagation in Tissues with Applications in Biology and Medicine. World Scientific; 2012. 10.1080/00107514.2013.810670
[4] Kak AC, Slaney M. Principles of Computerized Tomographic Imaging. Society for Industrial and Applied Mathematics; 2001. 10.1137/1.9780898719277
[5] Colas J-F, Sharpe J. Live optical projection tomography. Organogenesis 2009;5:211–16. doi:10.4161/org.5.4.10426.
[6] Power RM, Huisken J. A guide to light-sheet fluorescence microscopy for multiscale imaging. Nat Method 2017;14:360–73. doi:10.1038/nmeth.4224.
[7] Strobl F, Schmitz A, Stelzer EHK. Improving your four-dimensional image: traveling through a decade of light-sheet-based fluorescence microscopy research. Nat Protoc 2017;12:1103–9. doi:10.1038/nprot.2017.028.
[8] Girkin JM, Carvalho MT. The light-sheet microscopy revolution. J Opt 2018;20:53002. doi:10.1088/2040-8986/aab58a.
[9] Olarte OE, Andilla J, Gualda EJ, Loza-Alvarez P. Light-sheet microscopy: a tutorial. Adv Opt Photonics 2018;10:111. doi:10.1364/AOP.10.000111.
[10] Biggs DS. 3D deconvolution microscopy. Curr Prot Cytomet 2010:1–20. doi:10.1002/0471142956.cy1219s52.
[11] Hillman EM, Voleti V, Li W, Yu H. Light-sheet microscopy in neuroscience. Annu Rev Neurosci 2019;42:295–313. doi:10.1146/annurev-neuro-070918-050357.
[12] Wan Y, McDole K, Keller PJ. Light-sheet microscopy and its potential for understanding developmental processes. Annu Rev Cell Dev Biol 2019;35:1–27. doi:10.1146/annurev-cellbio-100818-125311.
[13] Albert-Smet I, Marcos-Vidal A, Vaquero JJ, Desco M, Muñoz Barrutia A, Ripoll J. Applications of light-sheet microscopy in microdevices. Front Neuroanat 2019;13:1–15. doi:10.3389/fnana.2019.00001.
[14] Poola PK, Afzal MI, Yoo Y, Kim KH, Chung E. Light sheet microscopy for histopathology applications. Biomed Eng Lett 2019;9:279–91. doi:10.1007/s13534-019-00122-y.
[15] Rieckher M, Ancora SEPD, Liapis E, Zacharopoulos A, Ripoll J, Tavernarakis N, et al. Demonstrating improved multiple transport-mean-free-path imaging capabilities of light sheet microscopy in the quantification of fluorescence dynamics. Biotechnol J 2018;13:1–7. doi:10.1002/biot.201700419.
[16] de Medeiros G, Balázs B, Hufnagel L. Light-sheet imaging of mammalian development. Semin Cell Develop Biol 2016;55:148–55. doi:10.1016/j.semcdb.2015.11.001.
[17] Gustavsson A-K, Petrov PN, Moerner WE. Light sheet approaches for improved precision in 3d localization-based super-resolution imaging in mammalian cells. Opt Express 2018;26:13122. doi:10.1364/OE.26.013122.
[18] Berthet B, Maizel A. Light sheet microscopy and live imaging of plants. J Microsc 2016;263:158–64. doi:10.1111/jmi.12393.
[19] Chatterjee K, Pratiwi FW, Wu FCM, Chen P, Chen BC. Recent progress in light sheet microscopy for biological applications. Appl Spectrosc 2018;72:1137–69. doi:10.1177/0003702818778851.
[20] Sharpe J, Ahlgren U, Perry P, Hill B, Ross A, Hecksher-Sørensen J, Baldock R, Davidson D. Optical projection tomography as a tool for 3d microscopy and gene expression studies. Science 2002;296:541–5. doi:10.1126/science.1068206.
[21] Ripoll J, Nieto-Vesperinas M, Carminati R. Spatial resolution of diffuse photon density waves. J Opti Soc Am A 1999;16:1466. doi:10.1364/JOSAA.16.001466.
[22] Ripoll J, Meyer H, Garofalakis A. In vivo optical tomography: from diffusion to ballistic. Opt Mater 2009;31:1082–5. doi:10.1016/j.optmat.2007.12.021.
[23] Gualda EJ, Vale T, Almada P, Feijó JA, Martins GG, Moreno N. Openspinmicroscopy: an open-source integrated microscopy platform. Nat Method 2013;10:599–600. doi:10.1038/nmeth.2508.
[24] Vallejo Ramirez PP, Zammit J, Vanderpoorten O, et al. OptiJ: Open-source optical projection tomography of large organ samples. Sci Rep 2019;9:15693. https://doi.org/10.1038/s41598-019-52065-0.
[25] Bassi A, Fieramonti L, D'Andrea C, Mione M, Valentini G. In vivo label-free three-dimensional imaging of zebrafish vasculature with optical projection tomography. J Biomed Opt 2011;16:100502. doi:10.1117/1.3640808.
[26] Mayer J, Robert-Moreno A, Danuser R, Stein JV, Sharpe J, Swoger J. OPTISPIM: integrating optical projection tomography in light sheet microscopy extends specimen characterization to nonfluorescent contrasts. Opt Lett 2014;39:1053. doi:10.1364/ol.39.001053.

[27] Miao Q, Hayenga J, Meyer MG, Neumann T, Nelson AC, Seibel EJ. Resolution improvement in optical projection tomography by the focal scanning method. Opt Lett 2010;35:3363–5. doi:10.1364/OL.35.003363.

[28] Fauver M, Seibel EJ, Rahn JR, Meyer MG, Patten FW, Neumann T, et al. Three-dimensional imaging of single isolated cell nuclei using optical projection tomography. Opt Express 2005;13:4210. doi:10.1364/OPEX.13.004210.

[29] Chen L, Kumar S, Kelly D, Andrews N, Dallman MJ, French PMW, et al. Remote focal scanning optical projection tomography with an electrically tunable lens. Biomed Opt Express 2014;5:3367. doi:10.1364/boe.5.003367.

[30] Sakhalkar HS, Oldham M. Fast, high-resolution 3d dosimetry utilizing a novel optical-CT scanner incorporating tertiary telecentric collimation. Med Phys 2007;35:101–11. doi:10.1118/1.2804616.

[31] Ban S, Cho NH, Min E, Bae JK, Ahn Y, Shin S, et al. Label-free optical projection tomography for quantitative three-dimensional anatomy of mouse embryo. J Biophotonics 2019;12:1–6. doi:10.1002/jbio.201800481.

[32] Torres VC, Li C, He Y, Sinha L, Papavasiliou G, Sattar HA, et al. Angular restriction fluorescence optical projection tomography to localize micrometastases in lymph nodes. J Biomed Opt 2019;24:1. doi:10.1117/1.JBO.24.11.110501.

[33] Bassi A, Brida D, D'Andrea C, Valentini G, Cubeddu R, De Silvestri S, et al. Time-gated optical projection tomography. Opt Lett 2010;35:2732–4. doi:10.1364/OL.35.002732.

[34] Fieramonti L, Bassi A, Foglia EA, Pistocchi A, D'Andrea C, Valentini G, Cubeddu R, De Silvestri S, Cerullo G, Cotelli F. Time-gated optical projection tomography allows visualization of adult zebrafish internal structures. PLoS ONE 2012;7:e50744. doi:10.1371/journal.pone.0050744.

[35] Wang L, Jacques SL, Zheng L. MCML Monte carlo modeling of light transport in multi-layered tissues. Comput Methods Programs Biomed 1995;47:131–46. doi:10.1016/0169-2607(95)01640-F.

[36] Sinha L, Massanes F, Torres VC, Li C, Tichauer KM, Brankov JG. Comparison of time- and angular-domain scatter rejection in mesoscopic optical projection tomography: a simulation study. Biomed Opt Express 2019;10:747. doi:10.1364/boe.10.000747.

[37] Kellner M, Heidrich M, Beigel R, Lorbeer R-A, Knudsen L, Ripken T, et al. Imaging of the mouse lung with scanning laser optical tomography (SLOT). J Appl Physiol 2012;113:975–83. doi:10.1152/japplphysiol.00026.2012.

[38] Nolte L, Antonopoulos GC, Rämisch L, Heisterkamp A, Ripken T, Meyer H. Enabling second harmonic generation as a contrast mechanism for optical projection tomography (OPT) and scanning laser optical tomography (SLOT). Biomed Opt Express 2018;9:2627. doi:10.1364/BOE.9.002627.

[39] Fei P, Yu Z, Wang X, Lu PJ, Fu Y, He Z, et al. High dynamic range optical projection tomography (HDR-OPT). Opt Express 2012;20:8824. doi:10.1364/OE.20.008824.

[40] Trull AK, van der Horst J, van Vliet LJ, Kalkman J. Comparison of image reconstruction techniques for optical projection tomography. Appl Opt 2018;57:1874. doi:10.1364/ao.57.001874.

[41] Tran TN, Yamamoto K, Namita T, Kato Y, Shimizu K. Three-dimensional transillumination image reconstruction for small animal with new scattering suppression technique. Biomed Opt Express 2014;5:1321. doi:10.1364/BOE.5.001321.

[42] Walls JR, Sled JG, Sharpe J, Henkelman RM. Resolution improvement in emission optical projection tomography. Phys Med Biol 2007;52:2775–90. doi:10.1088/0031-9155/52/10/010.

[43] van der Horst J, Kalkman J. Image resolution and deconvolution in optical tomography. Opt Express 2016;24:24460. doi:10.1364/OE.24.024460.

[44] Trull AK, Horst JVD, Palenstijn WJ, Vliet LJV, Leeuwen TV, Kalkman J. Point spread function based image reconstruction in optical projection tomography. Phys Med Biol 2017;62:7784–97. doi:10.1088/1361-6560/aa8945.

[45] Koskela O, Montonen T, Belay B, Figueiras E, Pursiainen S, Hyttinen J. Gaussian light model in brightfield optical projection tomography. Sci Rep 2019;9:13934. doi:10.1038/s41598-019-50469-6.

[46] Darrell A, Meyer H, Marias K, Brady M, Ripoll J. Weighted filtered backprojection for quantitative fluorescence optical projection tomography. Phys Med Biol 2008;53:3863–81. doi:10.1088/0031-9155/53/14/010.

[47] Dong D, Zhu S, Qin C, Kumar V, Stein JV, Oehler S, et al. Automated recovery of the center of rotation in optical projection tomography in the presence of scattering. IEEE J Biomed Health Inform 2013;17:198–204. doi:10.1109/TITB.2012.2219588.

[48] Zhu S, Dong D, Birk UJ, Rieckher M, Tavernarakis N, Qu X, et al. Automated motion correction for in vivo optical projection tomography. IEEE Trans Med Imaging 2012;31:1358–71. doi:10.1109/TMI.2012.2188836.

[49] Ancora D, Battista DD, Giasafaki G, Psycharakis SE, Liapis E, Ripoll J, et al. Phase-retrieved tomography enables mesoscopic imaging of opaque tumor spheroids. Sci Rep 2017;7:11854. doi:10.1038/s41598-017-12193-x.

[50] Fieramonti L, Foglia EA, Malavasi S, D'Andrea C, Valentini G, Cotelli F, et al. Quantitative measurement of blood velocity in zebrafish with optical vector field tomography. J Biophotonics 2015;8:52–9. doi:10.1002/jbio.201300162.

[51] Zeng Y, Xiong K, Lu X, Feng G, Han D, Wu J. Laser doppler projection tomography. Opt Lett 2014;39:904. doi:10.1364/OL.39.000904.

[52] Haidekker MA. Optical transillumination tomography with tolerance against refraction mismatch. Comput Methods Programs Biomed 2005;80:225–35. doi:10.1016/j.cmpb.2005.09.002.

[53] Birk UJ, Darrell A, Konstantinides N, Sarasa-Renedo A, Ripoll J. Improved reconstructions and generalized filtered back projection for optical projection tomography. Appl Opt 2011;50:392. doi:10.1364/AO.50.000392.

[54] Reidt SL, O'Brien DJ, Wood K, MacDonald MP. Polarised light sheet tomography. Opt Express 2016;24:11239. doi:10.1364/OE.24.011239.

[55] Fang M, Dong D, Zeng C, Liang X, Yang X, Arranz A, et al. Polarization-sensitive optical projection tomography for muscle fiber imaging. Sci Rep 2016;6:1–8. doi:10.1038/srep19241.

[56] Arranz A, Dong D, Zhu S, Savakis C, Tian J, Ripoll J. In-vivo optical tomography of small scattering specimens: time-lapse 3d imaging of the head eversion process in drosophila melanogaster. Sci Rep 2015;4:7325. doi:10.1038/srep07325.

[57] Nguyen D, Marchand PJ, Planchette AL, Nilsson J, Sison M, Extermann J, et al. Optical projection tomography for rapid whole mouse brain imaging. Biomed Opt Express 2017;8:5637. doi:10.1364/boe.8.005637.

[58] Lee KJ, Calder GM, Hindle CR, Newman JL, Robinson SN, Avondo JJ, et al. Macro optical projection tomography for large scale 3d imaging of plant structures and gene activity. J Exp Bot 2017;68:527–38. doi:10.1093/jxb/erw452.

[59] Chen L, McGinty J, Taylor HB, Bugeon L, Lamb JR, Dallman MJ, et al. Incorporation of an experimentally determined MTF for spatial frequency filtering and deconvolution during optical projection tomography reconstruction. Opt Express 2012;20:7323. doi:10.1364/OE.20.007323.

[60] Arranz A, Dong D, Zhu S, Rudin M, Tsatsanis C, Tian J, et al. Helical optical projection tomography. Opt Express 2013;21:25912. doi:10.1364/OE.21.025912.

[61] Mappes T, Jahr N, Csaki A, Vogler N, Popp J, Fritzsche W. The invention of immersion ultramicroscopy in 1912-the birth of nanotechnology? Angewandte Chemie - International Edition 2012;51:11208–12. doi:10.1002/anie.201204688.

[62] Siedentopf H, Zsigmondy R. Uber sichtbarmachung und größenbestimmung ultramikoskopischer teilchen, mit besonderer anwendung auf goldrubingläser. Ann Phys 1902;315:1–39. doi:10.1002/andp.19023150102.

[63] Voie AH, Burns DH, Spelman FA. Orthogonal-plane fluorescence optical sectioning: three-dimensional imaging of macroscopic biological specimens. J Microsc 1993;170:229–36. doi:10.1111/j.1365-2818.1993.tb03346.x.

[64] Fuchs E, Jaffe J, Long R, Azam F. Thin laser light sheet microscope for microbial oceanography. Opt Express 2002;10:145. doi:10.1364/OE.10.000145.

[65] Huisken J. Optical sectioning deep inside live embryos by selective plane illumination microscopy. Science 2004;305:1007–9. doi:10.1126/science.1100035.

[66] Keller PJ, Schmidt AD, Wittbrodt J, Stelzer EH. Reconstruction of zebrafish early embryonic development by scanned light sheet microscopy. Science 2008;322:1065–9. doi:10.1126/science.1162493.

[67] Truong TV, Supatto W, Koos DS, Choi JM, Fraser SE. Deep and fast live imaging with two-photon scanned light-sheet microscopy. Nat Method 2011;8:757–60. doi:10.1038/nmeth.1652.

[68] Huisken J, Stainier DYR. Even fluorescence excitation by multidirectional selective plane illumination microscopy (mSPIM). Opt Lett 2007;32:2608. doi:10.1364/ol.32.002608.

[69] Dodt H-U, Leischner U, Schierloh A, Jährling N, Mauch CP, Deininger K, et al. Ultramicroscopy: three-dimensional visualization of neuronal networks in the whole mouse brain. Nat Methods 2007;4:331–6. doi:10.1038/nmeth1036.

[70] Swoger J, Verveer P, Greger K, Huisken J, Stelzer EH. Multi-view image fusion improves resolution in three-dimensional microscopy. Opt Express 2007;15:8029. doi:10.1364/oe.15.008029.

[71] Krzic U, Gunther S, Saunders TE, Streichan SJ, Hufnagel L. Multiview light-sheet microscope for rapid in toto imaging. Nat Methods 2012;9:730–3. doi:10.1038/nmeth.2064.

[72] Tomer R, Khairy K, Amat F, Keller PJ. Quantitative high-speed imaging of entire developing embryos with simultaneous multiview light-sheet microscopy. Nat Method 2012;9:755–63. doi:10.1038/nmeth.2062.

[73] Chhetri RK, Amat F, Wan Y, Höckendorf B, Lemon WC, Keller PJ. Whole-animal functional and developmental imaging with isotropic spatial resolution. Nat Methods 2015;12:1171–8. doi:10.1038/nmeth.3632.

[74] He J, Huisken J. Image quality guided smart rotation improves coverage in microscopy. Nat Commun 2020;11:150. doi:10.1038/s41467-019-13821-y.

[75] Fei P, Nie J, Lee J, Ding Y, Li S, Zhang H, et al. Subvoxel light-sheet microscopy for high-resolution high-throughput volumetric imaging of large biomedical specimens. Adv Photon 2019;1:1. doi:10.1117/1.ap.1.1.016002.

[76] Nie J, Liu S, Yu T, Li Y, Ping J, Wan P, et al. Fast, 3d isotropic imaging of whole mouse brain using multiangle resolved subvoxel SPIM. Adv Sci 2020;7:1901891. doi:10.1002/advs.201901891.

[77] Sancataldo G, Gavryusev V, de Vito G, Turrini L, Locatelli M, Fornetto C, et al. Flexible multi-beam light-sheet fluorescence microscope for live imaging without striping artifacts. Front Neuroanat 2019;13:1–8. doi:10.3389/fnana.2019.00007.

[78] Calisesi G, Castriotta M, Candeo A, Pistocchi A, D'Andrea C, Valentini G, et al. Spatially modulated illumination allows for light sheet fluorescence microscopy with an incoherent source and compressive sensing. Biomed Opt Express 2019;10:5776. doi:10.1364/BOE.10.005776.

[79] Taylor MA, Vanwalleghem GC, Favre-Bulle IA, Scott EK. Diffuse light-sheet microscopy for stripe-free calcium imaging of neural populations. J Biophotonics 2018;11:1–9. doi:10.1002/jbio.201800088.

[80] Vinegoni C, Razansky D, Figueiredo J-L, Nahrendorf M, Ntziachristos V, Weissleder R. Normalized born ratio for fluorescence optical projection tomography. Opt Lett 2009;34:319. doi:10.1364/OL.34.000319.

[81] Mayer J, Robert-Moreno A, Sharpe J, Swoger J. Attenuation artifacts in light sheet fluorescence microscopy corrected by OPTiSPIM. Light 2018;7. doi:10.1038/s41377-018-0068-z.

[82] Fahrbach FO, Rohrbach A. Propagation stability of self-reconstructing bessel beams enables contrast-enhanced imaging in thick media. Nat Commun 2012;3:632. doi:10.1038/ncomms1646.

[83] Fahrbach FO, Simon P, Rohrbach A. Microscopy with self-reconstructing beams. Nat Photon 2010;4:780–5. doi:10.1038/nphoton.2010.204.

[84] Planchon TA, Gao L, Milkie DE, Davidson MW, Galbraith JA, Galbraith CG, et al. Rapid three-dimensional isotropic imaging of living cells using bessel beam plane illumination. Nat Method 2011;8:417–23. doi:10.1038/nmeth.1586.

[85] Olarte OE, Licea-Rodriguez J, Palero Ja, Gualda EJ, Artigas D, Mayer J, et al. Image formation by linear and nonlinear digital scanned light-sheet fluorescence mi-

croscopy with gaussian and bessel beam profiles. Biomed Opt Express 2012;3:1492. doi:10.1364/BOE.3.001492.
[86] Fahrbach FO, Gurchenkov V, Alessandri K, Nassoy P, Rohrbach A. Light-sheet microscopy in thick media using scanned bessel beams and two-photon fluorescence excitation. Opt Express 2013;21:13824. doi:10.1364/oe.21.013824.
[87] Escobet-Montalbán A, Gasparoli FM, Nylk J, Liu P, Yang Z, Dholakia K. Three-photon light-sheet fluorescence microscopy. Opt Lett 2018;43:5484. doi:10.1364/OL.43.005484.
[88] Jia H, Yu X, Yang Y, Zhou X, Yan S, Liu C, et al. Axial resolution enhancement of light-sheet microscopy by double scanning of bessel beam and its complementary beam. J Biophoton 2019;12:1–10. doi:10.1002/jbio.201800094.
[89] Vettenburg T, Dalgarno HI, Nylk J, Coll-Lladó C, Ferrier DE, Čižmár T, et al. Light-sheet microscopy using an airy beam. Nat Method 2014;11:541–4. doi:10.1038/nmeth.2922.
[90] Chen BC, Legant WR, Wang K, Shao L, Milkie DE, Davidson MW, et al. Lattice light-sheet microscopy: imaging molecules to embryos at high spatiotemporal resolution. Science 2014;346. doi:10.1126/science.1257998.
[91] Chang B-J, Kittisopikul M, Dean KM, Roudot P, Welf ES, Fiolka R. Universal light-sheet generation with field synthesis. Nat Method 2019;16:235–8. doi:10.1038/s41592-019-0327-9.
[92] Gao L. Optimization of the excitation light sheet in selective plane illumination microscopy. Biomed Opt Express 2015;6:881. doi:10.1364/BOE.6.000881.
[93] Remacha E, Friedrich L, Vermot J, Fahrbach FO. How to define and optimize axial resolution in light-sheet microscopy: a simulation-based approach. Biomed Opt Express 2020;11:8. doi:10.1364/BOE.11.000008.
[94] Smith AM, Mancini MC, Nie S. Second window for in vivo imaging. Nat Nanotechnol 2009;4:710–11. doi:10.1038/nnano.2009.326.
[95] Hong G, Diao S, Chang J, Antaris AL, Chen C, Zhang B, et al. Through-skull fluorescence imaging of the brain in a new near-infrared window. Nat Photon 2014;8:723–30. doi:10.1038/nphoton.2014.166.
[96] Wang F, Wan H, Ma Z, Zhong Y, Sun Q, Tian Y, et al. Light-sheet microscopy in the near-infrared II window. Nat Method 2019;16:545–52. doi:10.1038/s41592-019-0398-7.
[97] Silvestri L, Bria A, Sacconi L, Iannello G, Pavone FS. Confocal light sheet microscopy: micron-scale neuroanatomy of the entire mouse brain. Opt Express 2012;20:20582. doi:10.1364/oe.20.020582.
[98] Dean KM, Fiolka R. Uniform and scalable light-sheets generated by extended focusing. Opt Express 2014;22:26141. doi:10.1364/OE.22.026141.
[99] Dean KM, Roudot P, Welf ES, Danuser G, Fiolka R. Deconvolution-free subcellular imaging with axially swept light sheet microscopy. Biophys J 2015;108:2807–15. doi:10.1016/j.bpj.2015.05.013.
[100] Chakraborty T, Driscoll MK, Jeffery E, Murphy MM, Roudot P, Chang B-J, et al. Light-sheet microscopy of cleared tissues with isotropic, subcellular resolution. Nat Method 2019;16:1109–13. doi:10.1038/s41592-019-0615-4.
[101] Medeiros GD, Norlin N, Gunther S, Albert M, Panavaite L, Fiuza U-M, et al. Confocal multiview light-sheet microscopy. Nat Commun 2015;6:8881. doi:10.1038/ncomms9881.
[102] Ping J, Zhao F, Nie J, Yu T, Zhu D, Liu M, et al. Propagating-path uniformly scanned light sheet excitation microscopy for isotropic volumetric imaging of large specimens. J Biomed Opt 2019;24:1. doi:10.1117/1.jbo.24.8.086501.
[103] Meinert T, Rohrbach A. Light-sheet microscopy with length-adaptive bessel beams. Biomed Opt Express 2019;10:670. doi:10.1364/boe.10.000670.
[104] Nylk J, McCluskey K, Preciado MA, Mazilu M, Yang Z, Gunn-Moore FJ, et al. Light-sheet microscopy with attenuation-compensated propagation-invariant beams. Sci Adv 2018;4:eaar4817. doi:10.1126/sciadv.aar4817.
[105] Fahrbach FO, Voigt FF, Schmid B, Helmchen F, Huisken J. Rapid 3d light-sheet microscopy with a tunable lens. Opt Express 2013;21:21010. doi:10.1364/OE.21.021010.
[106] Duocastella M, Sancataldo G, Saggau P, Ramoino P, Bianchini P, Diaspro A. Fast inertia-free volumetric light-sheet microscope. ACS Photon 2017;4:1797–804. doi:10.1021/acsphotonics.7b00382.
[107] Wu Y, Ghitani A, Christensen R, Santella A, Du Z, Rondeau G, et al. Inverted selective plane illumination microscopy (iSPIM) enables coupled cell identity lineaging and neurodevelopmental imaging in caenorhabditis elegans. Proc Natl Acad Sci USA 2011;108:17708–13. doi:10.1073/pnas.1108494108.
[108] Strnad P, Gunther S, Reichmann J, Krzic U, Balazs B, de Medeiros G, et al. Inverted light-sheet microscope for imaging mouse pre-implantation development. Nat Method 2016;13:139–42. doi:10.1038/nmeth.3690.
[109] Wu Y, Wawrzusin P, Senseney J, Fischer RS, Christensen R, Santella A, et al. Spatially isotropic four-dimensional imaging with dual-view plane illumination microscopy. Nat Biotechnol 2013;31:1032–8. doi:10.1038/nbt.2713.
[110] Kumar A, Wu Y, Christensen R, Chandris P, Gandler W, McCreedy E, et al. Dual-view plane illumination microscopy for rapid and spatially isotropic imaging. Nat Protoc 2014;9:2555–73. doi:10.1038/nprot.2014.172.
[111] Theer P, Dragneva D, Knop M. πSPIM: high NA high resolution isotropic light-sheet imaging in cell culture dishes. Sci Rep 2016;6:1–9. doi:10.1038/srep32880.
[112] Migliori B, Datta MS, Dupre C, Apak MC, Asano S, Gao R, et al. Light sheet theta microscopy for rapid high-resolution imaging of large biological samples. BMC Biol 2018;16:1–19. doi:10.1186/s12915-018-0521-8.
[113] McGorty R, Liu H, Kamiyama D, Dong Z, Guo S, Huang B. Open-top selective plane illumination microscope for conventionally mounted specimens. Opt Express 2015;23:16142. doi:10.1364/oe.23.016142.
[114] Glaser AK, Reder NP, Chen Y, Yin C, Wei L, Kang S, et al. Multi-immersion open-top light-sheet microscope for high-throughput imaging of cleared tissues. Nat Commun 2019;10:1–8. doi:10.1038/s41467-019-10534-0.
[115] Glaser AK, Reder NP, Chen Y, McCarty EF, Yin C, Wei L, et al. Light-sheet microscopy for slide-free non-destructive pathology of large clinical specimens. Nat Biomed Eng 2017;1. doi:10.1038/s41551-017-0084.
[116] Barner LA, Glaser AK, True LD, Reder NP, Liu JTC. Solid immersion meniscus lens (SIMlens) for open-top light-sheet microscopy. Opt Lett 2019;44:4451. doi:10.1364/ol.44.004451.
[117] Mcgorty R, Xie D, Huang B. High-NA open-top selective-plane illumination microscopy for biological imaging. Opt Express 2017;25:17798. doi:10.1364/OE.25.017798.
[118] Holekamp TF, Turaga D, Holy TE. Fast three-dimensional fluorescence imaging of activity in neural populations by objective-coupled planar illumination microscopy. Neuron 2008;57:661–72. doi:10.1016/j.neuron.2008.01.011.
[119] Meddens MBM, Liu S, Finnegan PS, Edwards TL, James CD, Lidke KA. Single objective light-sheet microscopy for high-speed whole-cell 3d super-resolution. Biomed Opt Express 2016;7:2219. doi:10.1364/BOE.7.002219.
[120] Galland R, Grenci G, Aravind A, Viasnoff V, Studer V, Sibarita JB. 3D high-and super-resolution imaging using single-objective SPIM. Nat Method 2015;12:641–4. doi:10.1038/nmeth.3402.
[121] Gebhardt JCM, Suter DM, Roy R, Zhao ZW, Chapman AR, Basu S, et al. Single-molecule imaging of transcription factor binding to DNA in live mammalian cells. Nat Method 2013;10:421–6. doi:10.1038/nmeth.2411.
[122] Dunsby C. Optically sectioned imaging by oblique plane microscopy. Opt Express 2008;16:20306. doi:10.1364/OE.16.020306.
[123] Botcherby EJ, Juškaitis R, Booth MJ, Wilson T. An optical technique for remote focusing in microscopy. Opt Commun 2008;281:880–7. doi:10.1016/j.optcom.2007.10.007.
[124] Smith CW, Botcherby EJ, Wilson T. Resolution of oblique-plane images in sectioning microscopy. Opt Express 2011;19:2662. doi:10.1364/OE.19.002662.
[125] Yang B, Chen X, Wang Y, Feng S, Pessino V, Stuurman N, et al. Epi-illumination SPIM for volumetric imaging with high spatial-temporal resolution. Nat Method 2019;16:501–4. doi:10.1038/s41592-019-0401-3.
[126] Kim J, Wojcik M, Wang Y, Moon S, Zin EA, Marnani N, et al. Oblique-plane single-molecule localization microscopy for tissues and small intact animals. Nat Method 2019;16:853–7. doi:10.1038/s41592-019-0510-z.
[127] Alfred Millett-Sikking, & Andrew York. (2019, August 23). AndrewGYork/high_na_single_objective_lightsheet: Work-in-progress (Version 0.0.2). Zenodo. http://doi.org/10.5281/zenodo.3376243.
[128] Hoffmann M, Judkewitz B. Diffractive oblique plane microscopy. Optica 2019;6:1166. doi:10.1364/optica.6.001166.
[129] Sikkel MB, Kumar S, Maioli V, Rowlands C, Gordon F, Harding SE, et al. High speed sCMOS-based oblique plane microscopy applied to the study of calcium dynamics in cardiac myocytes. J Biophoton 2016;9:311–23. doi:10.1002/jbio.201500193.
[130] Fahrbach FO, Voigt FF, Schmid B, Helmchen F, Huisken J. Rapid 3d light-sheet microscopy with a tunable lens. Opt Express 2013;21:21010. doi:10.1364/oe.21.021010.
[131] Dwyer PJ, DiMarzio CA, Zavislan JM, Fox WJ, Rajadhyaksha M. Confocal reflectance theta line scanning microscope for imaging human skin in vivo. Opt Lett 2006;31:942. doi:10.1364/OL.31.000942.
[132] Bouchard MB, Voleti V, Mendes CS, Lacefield C, Grueber WB, Mann RS, et al. Swept confocally-aligned planar excitation (SCAPE) microscopy for high-speed volumetric imaging of behaving organisms. Nat Photon 2015;9:113–19. doi:10.1038/nphoton.2014.323.
[133] Kumar M, Kishore S, Nasenbeny J, McLean DL, Kozorovitskiy Y. Integrated one- and two-photon scanned oblique plane illumination (SOPi) microscopy for rapid volumetric imaging. Opt Express 2018;26:13027. doi:10.1364/OE.26.013027.
[134] Shin Y, Kim D, Kwon HS. Oblique scanning 2-photon light-sheet fluorescence microscopy for rapid volumetric imaging. J Biophoton 2018;11:e201700270. doi:10.1002/jbio.201700270.
[135] Voleti V, Patel KB, Li W, Campos CP, Bharadwaj S, Yu H, et al. Real-time volumetric microscopy of in vivo dynamics and large-scale samples with SCAPE 2.0. Nat Method 2019;16:1054–62. doi:10.1038/s41592-019-0579-4.
[136] Kumar M, Kozorovitskiy Y. Tilt-invariant scanned oblique plane illumination microscopy for large-scale volumetric imaging. Opt Lett 2019;44:1706. doi:10.1364/ol.44.001706.
[137] Santi PA. Light sheet fluorescence microscopy. J Histochem Cytochem 2011;59:129–38. doi:10.1369/0022155410394857.
[138] White RM, Sessa A, Burke C, Bowman T, LeBlanc J, Ceol C, Bourque C, Dovey M, Goessling W, Burns CE, Zon LI. Transparent adult zebrafish as a tool for in vivo transplantation analysis. Cell Stem Cell 2008;2:183–9. doi:10.1016/j.stem.2007.11.002.
[139] Wan P, Zhu J, Xu J, Li Y, Yu T, Zhu D. Evaluation of seven optical clearing methods in mouse brain. Neurophotonics 2018;5:1. doi:10.1117/1.nph.5.3.035007.
[140] Susaki EA, Ueda HR. Whole-body and whole-organ clearing and imaging techniques with single-cell resolution: toward organism-level systems biology in mammals. Cell Chem Biol 2016;23:137–57. doi:10.1016/j.chembiol.2015.11.009.
[141] Reynaud EG, Peychl J, Huisken J, Tomancak P. Guide to light-sheet microscopy for adventurous biologists. Nat Methods 2014;12:30–4. doi:10.1038/nmeth.3222.
[142] Flood P, Kelly R, Gutiérrez-Heredia L, Reynaud E. ZEISS lightsheet Z.1 sample preparation. Jena, Germany: Carl Zeiss Microscopy GmbH;; 2013.
[143] Berndt F, Shah G, Power RM, Brugués J, Huisken J. Dynamic and non-contact 3d sample rotation for microscopy. Nat Commun 2018;9:1–7. doi:10.1038/s41467-018-07504-3.
[144] Logan SL, Dudley C, Baker RP, Taormina MJ, Hay EA, Parthasarathy R. Automated high-throughput light-sheet fluorescence microscopy of larval zebrafish. PLoS ONE 2018;13:1–14. doi:10.1371/journal.pone.0198705.

[145] Kaufmann A, Mickoleit M, Weber M, Huisken J. Multilayer mounting enables long-term imaging of zebrafish development in a light sheet microscope. Development 2012;139:3242–7. doi:10.1242/dev.082586.
[146] Yang Z, Piksarv P, Ferrier DE, Gunn-Moore FJ, Dholakia K. Macro-optical trapping for sample confinement in light sheet microscopy. Biomed Opt Express 2015;6:2778. doi:10.1364/boe.6.002778.
[147] Kashekodi AB, Meinert T, Michiels R, Rohrbach A. Miniature scanning light-sheet illumination implemented in a conventional microscope. Biomed Opt Express 2018;9:4263. doi:10.1364/boe.9.004263.
[148] Yang Z, Cole KLH, Qiu Y, Somorjai IML, Wijesinghe P, Nylk J, et al. Light sheet microscopy with acoustic sample confinement. Nat Commun 2019;10:669. doi:10.1038/s41467-019-08514-5.
[149] de Medeiros G, Kromm D, Balazs B, Norlin N, Günther S, Izquierdo E, et al. Cell and tissue manipulation with ultrashort infrared laser pulses in light-sheet microscopy. Sci Rep 2020;10:1942. doi:10.1038/s41598-019-54349-x.
[150] Gualda E, Moreno N, Tomancak P, Martins GG. Going "open" with mesoscopy: a new dimension on multi-view imaging. Protoplasma 2014;251:363–72. doi:10.1007/s00709-013-0599-3.
[151] Owens B. The microscope makers. Nature 2017;551:659–62. doi:10.1038/d41586-017-07528-7.
[152] Pitrone PG, Schindelin J, Stuyvenberg L, Preibisch S, Weber M, Eliceiri KW, et al. OpenSPIM: an open-access light-sheet microscopy platform. Nat Method 2013;10:598–9. doi:10.1038/nmeth.2507.
[153] Edelstein A, Amodaj N, Hoover K, Vale R, Stuurman N. Computer control of microscopes using manager. Current Protocols in Molecular Biology. Hoboken, NJ, USA: John Wiley & Sons, Inc.; 2010. 10.1002/0471142727.mb1420s92
[154] Edelstein AD, Tsuchida MA, Amodaj N, Pinkard H, Vale RD, Stuurman N. Advanced methods of microscope control using μmanager software. J Biol Method 2014;1:10. doi:10.14440/jbm.2014.36.
[155] Schindelin J, Arganda-Carreras I, Frise E, Kaynig V, Longair M, Pietzsch T, et al. Fiji: an open-source platform for biological-image analysis. Nat Method 2012;9:676–82. doi:10.1038/nmeth.2019.
[156] Aakhte M, Akhlaghi EA, Müller HAJ. SSPIM: A beam shaping toolbox for structured selective plane illumination microscopy. Sci Rep 2018;8:1–12. doi:10.1038/s41598-018-28389-8.
[157] Gualda EJ, Pereira H, Vale T, Estrada MF, Brito C, Moreno N. SPIM-Fluid: open source light-sheet based platform for high-throughput imaging. Biomed Opt Express 2015;6:4447. doi:10.1364/BOE.6.004447.
[158] Voigt FF, Kirschenbaum D, Platonova E, Pagès S, Campbell RAA, Kastli R, et al. The mesoSPIM initiative: open-source light-sheet microscopes for imaging cleared tissue. Nat Methods 2019:577122. doi:10.1038/s41592-019-0554-0.
[159] Jahr W, Schmid B, Weber M, Huisken J. EduSPIM: light sheet microscopy in the museum. PLoS ONE 2016;11:e0161402. doi:10.1371/journal.pone.0161402.
[160] Royer LA, Lemon WC, Chhetri RK, Keller PJ. A practical guide to adaptive light-sheet microscopy. Nat Protoc 2018;13:2462–500. doi:10.1038/s41596-018-0043-4.
[161] Becker K, Saghafi S, Pende M, Sabdyusheva-Litschauer I, Hahn CM, Foroughipour M, et al. Deconvolution of light sheet microscopy recordings. Sci Rep 2019;9:17625. doi:10.1038/s41598-019-53875-y.
[162] Alfred Millett-Sikking, Nathaniel H. Thayer, Adam Bohnert, & Andrew G. York. (2018, January 11). calico/remote_refocus: Pre-print (Version v0.1). Zenodo. http://doi.org/10.5281/zenodo.1146084.
[163] Weigert M, Subramanian K, Bundschuh ST, Myers EW, Kreysing M. Biobeam multiplexed wave-optical simulations of light-sheet microscopy. PLoS Comput Biol 2018;14:e1006079. doi:10.1371/journal.pcbi.1006079.
[164] Prahl SA. A monte carlo model of light propagation in tissue. In: Mueller GJ, Sliney DH, Potter RF, editors. Dosimetry of Laser Radiation in Medicine and Biology, vol. 10305; 1989. p. 1030509. 10.1117/12.2283590
[165] Liu A, Xiao W, Li R, Liu L, Chen L. Comparison of optical projection tomography and light-sheet fluorescence microscopy. J Microsc 2019;275:3–10. doi:10.1111/jmi.12796.
[166] Bassi A, Schmid B, Huisken J. Optical tomography complements light sheet microscopy for in toto imaging of zebrafish development. Development 2015;142:1016–20. doi:10.1242/dev.116970.
[167] Rieckher M, Birk UJ, Meyer H, Ripoll J, Tavernarakis N. Microscopic optical projection tomography in vivo. PLoS ONE 2011;6:2–7. doi:10.1371/journal.pone.0018963.
[168] Jiang Y, Pu K. Molecular fluorescence and photoacoustic imaging in the second near-infrared optical window using organic contrast agents. Adv Biosyst 2018;2:1700262. doi:10.1002/adbi.201700262.
[169] Zubkovs V, Antonucci A, Schuergers N, Lambert B, Latini A, Ceccarelli R, et al. Spinning-disc confocal microscopy in the second near-infrared window (NIR-II). Sci Rep 2018;8:13770. doi:10.1038/s41598-018-31928-y.